

FREIE UNIVERSITÄT BERLIN  
DEPARTMENT OF PHYSICS

Master thesis

---

Majorana fermions  
in quantum wires  
and the influence of environment

---

*Written by:*  
Konrad Wölms

*Supervisor:*  
Prof. Karsten Flensberg  
Prof. Piet Brouwer

25. May 2012



# Contents

	page
<b>1 Introduction</b>	<b>5</b>
<b>2 Majorana Fermions</b>	<b>7</b>
2.1 Kitaev model . . . . .	9
2.2 Helical Liquids . . . . .	12
2.3 Spatially varying Zeeman fields . . . . .	14
2.3.1 Scattering matrix criterion . . . . .	16
2.4 Application of the criterion . . . . .	17
<b>3 Majorana qubits</b>	<b>21</b>
3.1 Structure of the Majorana Qubits . . . . .	21
3.2 General Dephasing . . . . .	22
3.3 Majorana 4-point functions . . . . .	24
3.4 Topological protection . . . . .	27
<b>4 Perturbative corrections</b>	<b>29</b>
4.1 Local perturbations . . . . .	29
4.1.1 Calculation of the correlation function . . . . .	30
4.1.2 Non-adiabatic effects of noise . . . . .	32
4.1.3 Uniform movement of the Majorana fermion . . . . .	34
4.2 Coupling between Majorana fermions . . . . .	36
4.2.1 Static perturbation . . . . .	36
4.3 Phonon mediated coupling . . . . .	39
4.3.1 Split Majorana Green function . . . . .	39
4.3.2 Phonon Coupling . . . . .	40
4.3.3 Self-Energy . . . . .	41
4.3.4 Self Energy in terms of local functions . . . . .	43
4.4 Calculation of $B$ . . . . .	44
4.4.1 General form for the electron Green function . . . . .	46
4.5 Calculation of $\Sigma$ . . . . .	46
<b>5 Summary</b>	<b>51</b>
<b>6 Acknowledgments</b>	<b>53</b>
<b>Bibliography</b>	<b>55</b>



# 1 Introduction

One of the fascinating aspects of condensed matter is the emergence of quasi-particles. These often describe the low energy behavior of complicated many-body systems extremely well and have long become an essential tool for the theoretical description of many condensed matter systems. Examples for quasi-particles are for instance the phonon, the Bloch-electron, the polariton or the magnon. All these examples obey Bose-Einstein or Fermi-Dirac statistics, exactly as elementary particles observed in nature do. It turns out that many-body systems seem to be even richer. There have been suggestions that low energy theories of some condensed matter systems will involve quasi-particles that obey so-called non-abelian statistics in contrast to fermionic or bosonic statistics. Those include the excitations in fractional quantum hall systems as well as Majorana bound states in topological superconductors. The latter are the ones with which we will be concerned in this thesis.

Since Majorana fermions are always related to so-called topological superconductors, we will first discuss what this means and when this phase of matter appears. Usually this involves heterostructure including a *s*-wave superconductor as well as semi-conductors with spin-orbit interaction and a strong Zeeman field. We are also going to discuss a method that does not involve spin-orbit coupling, but rather relies on spatially inhomogeneous magnetic fields.

Besides the non-abelian nature of their statistics, Majorana fermions also have a certain degree of protection against perturbations. This makes them interesting for potential applications in quantum computation. A large part of this thesis is going to be about the amount of this protection related to quantum information, in particular the protection of qubits that are built out of Majorana fermions.

The fundamental feature of Majorana fermions with regard to quantum information is that two Majorana fermions store a qubit non-locally. Non-local means that the wave functions of the Majorana fermions do not need any overlap at all in order to store the qubit and ideally they do not have any overlap. This leaves essentially two kinds of perturbations that can be investigated. The first kind includes perturbations that couple one or more Majorana fermions directly. Effects resulting from this sort of perturbation can be eliminated by taking the Majorana fermions far apart and the question that remains, is how fast the effect diminishes with increasing distance. The other kind of perturbations couples to one Majorana fermion only. Those effects are always present and do not vanish for large distances between the Majorana fermions. Yet these effects are different from the ones a localized electronic state experiences. We will look at perturbations of both kinds. Furthermore we will relate those effects to properties of the Majorana qubit.



## 2 Majorana Fermions

Majorana fermions are fermions, which are their own anti-particles. In second quantized form this means that the Majorana operators  $\gamma_i$  fulfill the relation

$$\gamma_i^\dagger = \gamma_i. \quad (2.1)$$

Together with the fermionic anti-commutation relations this implies that the Majorana fermions square to a constant. They are chosen to be normalized such that this constant is 1. Therefore we have the relations

$$\begin{aligned} \gamma_i^2 &= 1 \\ \{\gamma_i, \gamma_j\} &= 2\delta_{ij}. \end{aligned} \quad (2.2)$$

It is known that none of the elementary particles that constitute condensed matter systems fulfill these relations. On the other hand, when one thinks of quasi-particles for which creation and annihilation are similar, Bogoliubov quasi-particles from superconducting phases should come into mind. In fact, the particle-hole symmetry of those systems tells us the following relation between creation and annihilation operators:

$$b^\dagger(\varepsilon) = b(-\varepsilon). \quad (2.3)$$

This tells us that we might find the Majorana fermions we are looking for as zero energy states in superconducting phases.

Within superconducting systems, that allow for their excitations to contain particle and hole parts at the same time, we can now formally write a Majorana fermion that fulfills the equation (2.1) as

$$\gamma_i = \int dx \left( f_i(x) \Psi^\dagger(x) + f_i^*(x) \Psi(x) \right). \quad (2.4)$$

Their statistics from equation (2.2) now translate into

$$\begin{aligned} \int dx |f_i(x)|^2 &= 1 \\ \int dx (f_i^*(x) f_j(x) + f_j^*(x) f_i(x)) &= 0. \end{aligned} \quad (2.5)$$

For a lot of our discussions the above picture is going to be sufficient and will already contain the physics we are interested in. However, in a realistic model we of course need to include spin. We then have a Majorana fermion of the form

$$\gamma_i = \sum_s \int dx \left( f_{is}(x) \Psi_s^\dagger(x) + f_{is}^*(x) \Psi_s(x) \right). \quad (2.6)$$

## 2 Majorana Fermions

The analogue of equation (2.5) now also needs a sum over spin. We get

$$\begin{aligned} \sum_s \int dx |f_{is}(x)|^2 &= 1 \\ \sum_s \int dx (f_{is}^*(x)f_{js}(x) + f_{js}^*(x)f_{is}(x)) &= 0. \end{aligned} \quad (2.7)$$

It is sometimes advantageous to look at Majorana fermions in the Bogoliubov-spinor picture, which helps to investigate some of their basic properties in a simple single particle bra ket notation. This notation is well-suited for studying the effect of single particle potentials. We first write a Hamiltonian in the usual Bogoliubov way <sup>1</sup>

$$\mathcal{H} = \frac{1}{2} \int dx \Psi^\dagger(x) H(x) \Psi(x). \quad (2.8)$$

Here  $\Psi(x) = (\Psi(x), \Psi^\dagger(x))^T$ . Furthermore the Hamiltonian has to be written such that it is particle-hole symmetric. This means that there exists a particular particle-hole operator  $S_{\text{ph}}$ , which is related to the structure of  $\Psi(x)$ , such that  $\{S_{\text{ph}}, H\} = 0$  or equivalently

$$S_{\text{ph}} H S_{\text{ph}}^{-1} = -H. \quad (2.9)$$

The spinor solutions to  $H(x)$  will now yield solutions to the actual Hamiltonian, in particular for a spinor eigenstate  $|b\rangle = (g(x), h(x))$  the operator corresponding to the solution of the second quantized Hamiltonian  $\mathcal{H}$  is  $b^\dagger = \int dx \Psi^\dagger(g(x), h(x))^T$ .

Due to the particle-hole symmetry the spinor solutions will come in pairs with energies  $\pm E$ . If we have a solution for positive energy of the form

$$H|b+\rangle = E|b+\rangle, \quad (2.10)$$

we can apply  $S_{\text{ph}}$  to the equation to find

$$\begin{aligned} E S_{\text{ph}} |b+\rangle &= S_{\text{ph}} H |b+\rangle \\ &= S_{\text{ph}} H S_{\text{ph}}^{-1} S_{\text{ph}} |b+\rangle \\ &= -H S_{\text{ph}} |b+\rangle. \end{aligned} \quad (2.11)$$

We can now call  $S_{\text{ph}} |b+\rangle = |b-\rangle$  and have

$$H|b-\rangle = -E|b-\rangle. \quad (2.12)$$

It can be shown that the state  $|b-\rangle$  represents the operator  $b$ , if  $|b+\rangle$  represents  $b^\dagger$ . This means that the Majorana fermion has to be invariant under the particle-hole operator. In our case the particle-hole operator takes the form  $S_{\text{ph}} = \tau_x C$ , where  $C$  is the complex

---

<sup>1</sup>We will only use calligraphic letters in this section to make the distinction between spinor space in operator space more clear. Later on it will be clear from the context which picture we are using and we will not use calligraphic letters again.

conjugation operator. This tells us that the spinors that represent Majorana fermions will take the form  $|\gamma_i\rangle = (f_j^*(x), f_j(x))$ .

Furthermore we note that we can translate the second quantized picture to our first quantized one with the formulas

$$\begin{aligned}\langle a|b\rangle &= \{a, b^\dagger\} \\ \langle a|V|b\rangle &= \{a, [\mathcal{V}, b^\dagger]\}.\end{aligned}\quad (2.13)$$

In fact we could have also used this as a starting definition for going from second to first quantization instead of equation (2.8). The important part is simply that the whole Hamiltonian is bilinear in creation and annihilation operators, such that the right hand side of second line of equation (2.13) always yields a number not an operator. Note also that (2.13) gives 0 for  $\mathcal{V} = 1$ . This helps to ensure that (2.13) does not depend on the way the Hamiltonian is written, in particular whether we write  $c^\dagger c$  or  $1 - cc^\dagger$  for a given electronic state. Equation (2.13) also tells us that the Majorana states are normalized to two instead of one. It also tells us that Majorana fermions have a vanishing expectation value for all operators

$$\begin{aligned}\langle \gamma_j|V|\gamma_j\rangle &= \gamma_j \mathcal{V} \gamma_j + \mathcal{V} \gamma_j \gamma_j - \gamma_j \gamma_j \mathcal{V} - \gamma_j \mathcal{V} \gamma_j \\ &= 0.\end{aligned}\quad (2.14)$$

Another useful property to note is that the matrix elements of a hermitian operator between different Majorana fermions are purely imaginary. This can be seen as follows

$$\begin{aligned}\langle \gamma_1|V|\gamma_2\rangle^* &= \{\gamma_1, [\mathcal{V}, \gamma_2]\}^\dagger \\ &= \{[\gamma_2, \mathcal{V}], \gamma_1\} \\ &= -\{\gamma_1, [\mathcal{V}, \gamma_2]\} \\ &= -\langle \gamma_1|V|\gamma_2\rangle.\end{aligned}\quad (2.15)$$

## 2.1 Kitaev model

Now in order to begin the discussion on Majorana fermions, we will first have a brief look at the simplest example of a superconducting phase that supports Majorana fermions. Such a phase is called a topological superconductor and the first simple example for it was given by Kitaev [7]. Kitaev looked at a one-dimensional spinless  $p$ -wave superconductor of the form

$$H = \sum_j \left[ -w(c_j^\dagger c_{j+1} + \text{h.c.}) - \mu(c_j^\dagger c_j - \frac{1}{2}) + (\Delta^* c_{j+1}^\dagger c_j^\dagger + \text{h.c.}) \right]. \quad (2.16)$$

Mathematically we can always decompose ordinary fermion operators into Majorana operators that have the properties (2.1) and (2.2). This is achieved by

$$\begin{aligned}\gamma_{2j-1} &= e^{i\varphi} c_j^\dagger + e^{-i\varphi} c_j \\ \gamma_{2j} &= i e^{i\varphi} c_j^\dagger - i e^{-i\varphi} c_j,\end{aligned}\quad (2.17)$$

## 2 Majorana Fermions

where  $\varphi$  is an arbitrary phase. If we now write  $\Delta = |\Delta|e^{i\theta}$  and choose  $\varphi = \frac{\theta}{2}$  we obtain the Hamiltonian (2.16) in the form

$$H = \frac{i}{2} \sum_j [-\mu\gamma_{2j-1}\gamma_{2j} + (w + |\Delta|)\gamma_{2j}\gamma_{2j+1} + (-w + |\Delta|)\gamma_{2j-1}\gamma_{2j+1}]. \quad (2.18)$$

At the special point  $|\Delta| = w$  and  $\mu = 0$  the Hamiltonian takes the very simple form

$$H = iw \sum_j \gamma_{2j}\gamma_{2j+1}. \quad (2.19)$$

The important thing to note here is that the Majorana operators from different sites are paired, i.e.  $\gamma_{2j}$  and  $\gamma_{2j+1}$  are paired instead of  $\gamma_{2j-1}$  and  $\gamma_{2j}$ . Therefore the Majorana operators  $\gamma_1$  and  $\gamma_{2N}$  do not appear inside the Hamiltonian. Furthermore they are located at opposite ends of the wire and should therefore be regarded as physical objects even though they originate from the mathematical transformation (2.17). In his original article Kitaev then continues to argue that the two localized Majorana fermions may remain even away from this special point in parameter space. Those states will not be perfectly localized at one site anymore, but will have an exponential tail inside the wire. For sufficiently long wires this will not cause a splitting due to the overlap between the two Majorana fermions. Furthermore it is expected that Majorana fermions do not only appear at the ends of a wire, but always at the domain wall between a topological superconducting phase and a topological trivial phase. This includes the states at the ends of a topological superconducting wire, because the vacuum turns out to be topologically trivial. In order to have Majorana fermions this requires that different domain walls are far enough apart such that the Majorana fermions do not split.

The question now is how one can distinguish the topologically superconducting phase with Majorana fermions from the ordinary superconducting (or topologically trivial) phase. Kitaev also gave the first criterion to determine whether one is inside the topological phase. It is now assumed that the Hamiltonian of the system is written in the form

$$H = \frac{i}{4} \sum_{jm,\alpha\beta} B_{\alpha\beta}(m-j)\gamma_{\alpha m}\gamma_{\beta j}, \quad (2.20)$$

where  $m$  and  $j$  denote site indices and  $\alpha$  and  $\beta$  mark different Majorana fermions on the same site (for example Majorana fermions with different spin). Furthermore the matrix  $B$  is taken to be antisymmetric. As an example, we can write equation (2.18) in this form with  $B$  as

$$B_{\alpha\beta}(m-j) = [-\mu\delta_{m,j} + (w + |\Delta|)\delta_{m,j+1} + (-w + |\Delta|)\delta_{m-1,j+1}] \epsilon_{\alpha\beta}, \quad (2.21)$$

where  $\epsilon_{\alpha\beta}$  is the Levi-Civita-Symbol in two dimension. The so-called topological number of the superconductor is now given by

$$M(H) = \text{sgn}(\text{Pf}(B)). \quad (2.22)$$

When the topological number is 1 there are no Majorana fermions at the ends of the wire, if the number is  $-1$  there are. In general it is not feasible to calculate the pfaffian of a large matrix, especially analytically. Yet in writing equation (2.20) where the matrix  $B$  only depends on the difference of the indexes we already assumed that the system is translationally invariant. This is not essential for the form of the criterion as given in equation (2.22), but Kitaev showed that it can drastically simplify the calculation of  $M$ . We can now look at the quantity

$$\tilde{B}_{\alpha\beta}(q) = \sum_j e^{iqja} B_{\alpha\beta}(j), \quad (2.23)$$

where  $a$  is the lattice spacing. In terms of this matrix  $\tilde{B}$  the criterion can be shown to take the form

$$M(H) = \text{sgn}(\text{Pf}(\tilde{B}(0)))\text{sgn}(\text{Pf}(\tilde{B}(\pi/a))). \quad (2.24)$$

For the Kitaev model we find that  $\tilde{B}$  takes the form

$$\tilde{B}_{\alpha\beta}(q) = (-\mu + e^{-iqa}(w + |\Delta|) + e^{-i2qa}(-w + |\Delta|))\epsilon_{\alpha\beta}. \quad (2.25)$$

With this we find the topological number to be

$$M(H) = \text{sgn}((- \mu + 2|\Delta|)(- \mu - 2w)). \quad (2.26)$$

It can be seen that it is  $-1$  not only for the special point  $\mu = 0$ ,  $|\Delta| = w$  but also for a whole range of other parameter values.

To summarize, we will briefly discuss the relevance of Kitaev's model. In particular it would be interesting why one has to look at systems as exotic as a spinless  $p$ -wave superconductor in order to find Majorana fermion. We already argued earlier that we need superconductivity, in particular particle-hole symmetry, to have Majorana fermions. The problem is that particle-hole symmetry as it appears in ordinary  $s$ -wave superconductor relates electrons of different spin. Thus adding an electron with spin up is similar to removing one with spin down. Therefore adding and removing can never be the same in this scenario and we need  $p$ -wave order that pairs identical spins. Figure 2.1 illustrates this. This is the reason why all the other models which we will describe try to mimic a  $p$ -wave superconductor and their low energy behavior will be described by theories which are similar to Kitaev's model.

As for Kitaev's criterion for having a topological phase, it turns out that the simplified version of it is of limited use in practice. The reason for this is, that it only works for translationally invariant systems and the systems we use to mimic  $p$ -wave superconductivity may not have this property. Furthermore it is not suited to study the effect of non-translationally invariant perturbations. The original criterion (2.22) that does not rely on translational invariance can be used for numerical studies. The disadvantages are that it uses the full Hamiltonian and that it is not easy to calculate the pfaffian of a big matrix.

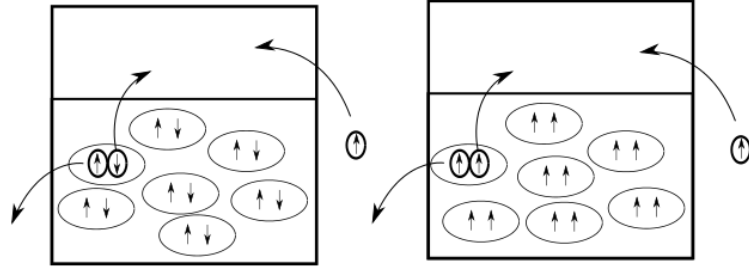


Figure 2.1: These sketches illustrate particle-hole symmetry. On the left hand side we see a superconductor where the Cooper-pairs form spin singlets. We see that in such a system removing a spin up electron from the system corresponds to creating a spin down excitation. Because the spin of the excitation has a different direction depending on whether a particle is added or removed, the system is not likely to support Majorana fermion quasi-particles. On the right hand side we see how this problem is solved, if we have a superconductor with spin polarized Cooper-pairs. Adding and removing an electron now yields a spin up excitation. This kind of system may therefore have a topologically nontrivial phase.

## 2.2 Helical Liquids

We will now briefly summarize ideas that explain a way to obtain an effective  $p$ -wave superconductor. Those were first presented by Oreg et al.[11] and Lutchyn et al. [9]. The idea is to induce superconductivity inside a semi-conducting quantum wire via ordinary  $s$ -wave proximity effect. In order to obtain  $p$ -wave order a Zeeman-field is included. The induced Zeeman splitting has to be large enough to leave only one spin direction below the chemical potential. The problem with this is that the spin-polarized band cannot be subject to the  $s$ -wave proximity effect. Now if the wire is subject to spin-orbit-interaction, it mixes the spin directions for different momenta. This allows for the lower band to be subject to the proximity effect and therefore we might end up having  $p$ -wave order since  $s$ -wave is unfavorable in a spin polarized system. Another way to look at it is as follows. The Spin orbit interaction displaces the dispersion of the different spin directions. The Zeeman field then causes them to anticross. If the chemical potential lies within the gap that opens that way, we have chiral low energy behavior. This situation is illustrated in figure 2.2.

The Hamiltonian for such a system can be written in the general form

$$\mathcal{H} = \frac{1}{2} \int dy \Psi^\dagger(y) H \Psi(y), \quad (2.27)$$

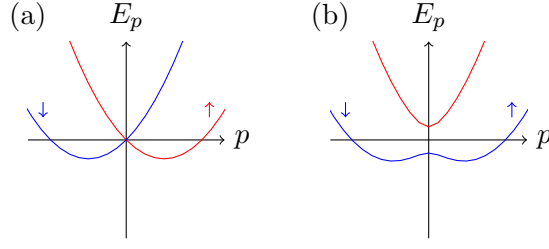


Figure 2.2: (a) shows how spin-orbit coupling in the absence of a Zeeman field displaces the bands for the different spin directions. In (b) we see how an added Zeeman field causes the bands to anticross. In the large  $p$  limit the spin orientation approaches the one of (a), because the momentum dependent spin orbit interaction dominates the constant Zeeman field. This way we obtain the helical nature of the low energy behavior, if the chemical potential falls into the energy gap.

with  $\Psi^\dagger = (\psi_\uparrow^\dagger, \psi_\downarrow^\dagger, \psi_\downarrow, -\psi_\uparrow)$ .  $H$  then takes the form

$$H \left( \frac{p^2}{2m} - \mu \right) \tau_z + up\sigma_z\tau_z + B\sigma_x + \Delta\tau_x. \quad (2.28)$$

The spectrum of this Hamiltonian can be found to be

$$E_p^2 = \xi_p^2 + u^2p^2 + B^2 + \Delta^2 \pm 2\sqrt{\Delta^2B^2 + \xi_p^2B^2 + u^2p^2\xi_p^2}. \quad (2.29)$$

Here we used the shortened notation  $\xi_p = \frac{p^2}{2m} - \mu$ . It was then shown that such a system is in the topological phase whenever

$$B^2 > \Delta^2 + \mu^2. \quad (2.30)$$

If one looks at the spectrum at  $p = 0$ , which takes the form

$$\begin{aligned} E^2 &= \mu^2 + B^2 + \Delta^2 \pm 2B\sqrt{\Delta^2 + \mu^2} \\ &= (B \pm \sqrt{\Delta^2 + \mu^2}), \end{aligned} \quad (2.31)$$

one finds that the point  $B^2 = \Delta^2 + \mu^2$  is precisely the point where the gap closes.

There are several things one should note about this model. First of all it is crucial for the result that the magnetic field is perpendicular to the spin-orbit coupling. Furthermore the result does not seem to depend on the spin-orbit coupling strength. Nevertheless spin-orbit coupling is crucial for the system, because it would otherwise not become superconducting. From equation (2.29) one can obtain that the system is not gapped for  $u = 0$ , which agrees with the physical intuition that  $s$ -wave proximity effect cannot affect perfectly spin-polarized bands.

### 2.3 Spatially varying Zeeman fields

It was suggested that spin-orbit coupling is not essential to having Majorana fermions [4]. Instead it seems to be sufficient if the Zeeman field is spatially inhomogeneous. The reason for that can easily be seen. We take a Hamiltonian of the form

$$H = \left( \frac{p^2}{2m} - \mu \right) \tau_z + \Delta \tau_x + \boldsymbol{\sigma} \cdot \mathbf{B}(y) \quad (2.32)$$

and for simplicity assume that the Zeeman field only varies within the  $x$ - $y$ -plane, we can now perform a  $y$ -dependent unitary transformation that aligns the B-field in the  $x$ -direction. The unitary transformation takes the form

$$U(y) = \exp(-i\varphi(y)\sigma_z/2), \quad (2.33)$$

where  $\varphi$  is the angle the  $x$ -axis makes with the  $B$ -field, starting from the  $x$ -axis and going clockwise. After this rotation the Hamiltonian takes the form

$$\begin{aligned} \tilde{H} &= U(y)HU^\dagger(y) \\ &= \left( \frac{p^2}{2m} - \mu \right) \tau_z + \Delta \tau_x + \sigma_x B(y) + H_1 + H_2. \end{aligned} \quad (2.34)$$

Here  $B = |\mathbf{B}|$  and  $H_1$  and  $H_2$  are corrections that result from the fact that  $U(y)$  does not commute with the kinetic part of the Hamiltonian. They take the form

$$H_1 = \left( \frac{\partial_y \varphi(y)}{4m} p + p \frac{\partial_y \varphi(y)}{4m} \right) \sigma_z \tau_z \quad (2.35)$$

and

$$H_2 = \frac{(\partial_y \varphi(y))^2}{8m}. \quad (2.36)$$

$H_1$  has the form of a space dependent spin-orbit interaction and  $H_2$  gives a space dependent correction to the chemical potential.

The easiest case one can image, is the case where  $\varphi(y) = \lambda y$  and  $|\mathbf{B}|$  is constant. This describes a Zeeman field that rotates as a function of  $y$  at a constant rate. For this particular choice of  $\varphi(y)$  we can simplify  $H_1$  such that  $\tilde{H}$  takes the form of equation (2.28) with  $u = \frac{\lambda}{2m}$  and the replacement  $\mu \rightarrow \mu - \frac{\lambda^2}{8m}$ . It is therefore clear that our geometry can in principle support Majorana fermions. The condition for this now takes the form

$$B^2 > \Delta^2 + \left( \mu - \frac{\lambda^2}{8m} \right). \quad (2.37)$$

The correction to  $\mu$  is also in favor of engineering the topological phase, because it allows for bigger chemical potentials. However, if we estimate  $\lambda$  to be around 100 nm and  $m$  to be about one tenth of the electron mass, we get a correction to the chemical of the order of 10  $\mu\text{eV}$ , which is rather small.

It remains to investigate to what extent we can find topological phases for field shapes that might be more realistic in a lab situation. We investigate geometries that resemble a

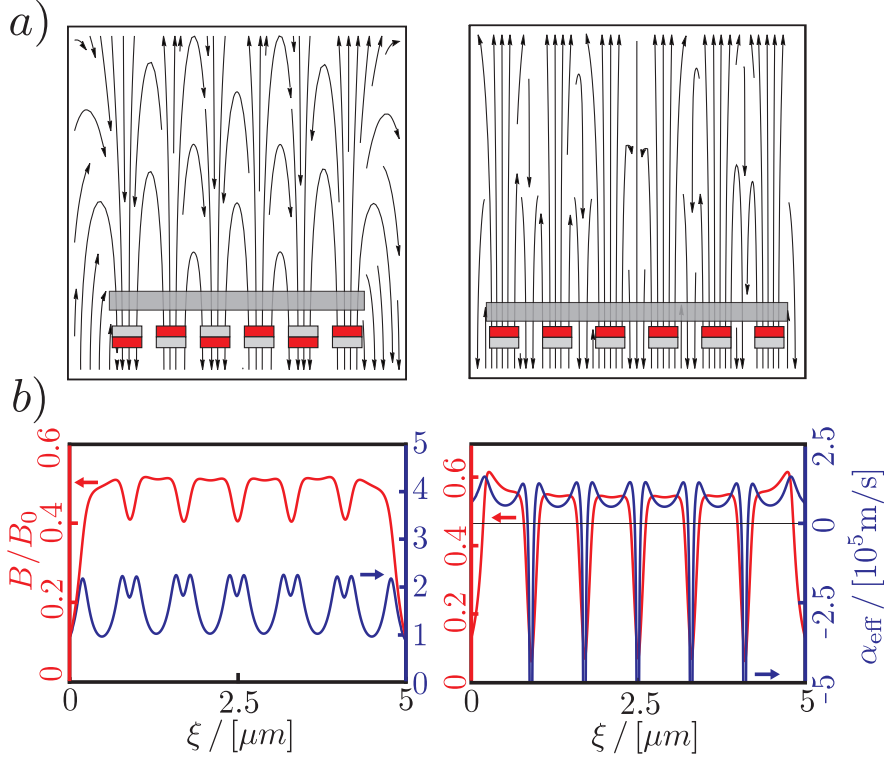


Figure 2.3: (a) Nanowires close to an array of magnets that either point in the alternating directions or in the same one. The field lines indicate the behavior of the magnetic field if the magnets are modeled as solenoids. (b) Effective spin-orbit strength and Zeeman field strength for both geometries depicted in (a).  $\xi$  denotes distance along the wire, and  $B_0$  is a characteristic field strength for an individual solenoid.

spatially uniform rotation of the Zeeman field. The situation we have in mind for this is an array of permanent magnets with alternating direction of magnetic field. This situation is depicted in figure 2.3 (a). Such an array could be produced by having the magnets be of different length, such that they have different hysteresis loops. Their magnetization could then be tuned to point the opposite way. Our model for this situation is going to be an array of solenoid fields. Figure 2.3 (a) also depicts the field lines of such a configuration and they seem to resemble the rotating behavior we would like. The magnets are modeled as solenoids. They have widths of 600 nm, heights of 330 nm and the gap between them is 200 nm. For the first configuration they are 100 nm away from the wire, for the second one they are only 50 nm away.

Since we now have a strong spatial dependence in our Hamiltonian, we cannot apply the simplified Kitaev criterion (2.24) to analytically analyze the topological phases of our geometry. We will therefore proceed numerically. One way this could be done is

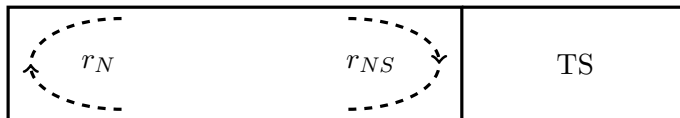


Figure 2.4: This illustrates how a perfectly reflecting topological superconductor denoted with TS in the figure, can give rise to bound states at its ends

by applying the unsimplified version of Kitaev's criterion, i.e. equation (2.22), to the Hamiltonian. In order to do this one would need an efficient way of calculating the pfaffian of a large matrix as it is provided in [12], for example. We, however, use an alternative criterion as described by Fulga et al. [5] to analyze whether or not we have a topological phase. We will now briefly summarize the idea behind this criterion.

### 2.3.1 Scattering matrix criterion

Instead of the Hamiltonian, this criterion analyzes the scattering matrix of the wire system in question. If the system is assumed to be long enough, such that it perfectly reflects every incoming particle, and a normal metal lead is attached, there can be bound states inside the lead. In a quasi-1D geometry one can easily get an idea how bound states and scattering are related. One imagines a particle moving towards one end of the wire. There it will get completely reflected and move to the other end where it gets reflected again. If it is in a bound state of the system it should still be in the same state after those two reflections. Moreover it should not have obtained any phase, otherwise it could interfere with itself. This tells us that the bound states are those, which have eigenvalue one under the consecutive application of the reflection matrices of both ends of the system. This can be formulated as

$$\text{Det}(1 - r_N r_{NS}) = 0. \quad (2.38)$$

The situation is depicted in figure 2.4.

Since Majorana fermions are zero energy bound states, the question is whether equation (2.38) can be fulfilled for zero energy. Due to particle-hole symmetry the form of the scattering matrix is very restricted at zero energy. In what follows all the scattering matrices are therefore assumed to be at zero energy. The normal reflection matrix will take the form

$$r_N = \begin{pmatrix} U_N & 0 \\ 0 & U_N^* \end{pmatrix} \quad (2.39)$$

and the one at the interface to the superconducting wire takes the form

$$r_{NS} \begin{pmatrix} r_{ee} & r_{eh} \\ r_{he} & r_{hh} \end{pmatrix}. \quad (2.40)$$

The latter one is additionally constrained by  $r_{eh} = r_{he}^*$  and  $r_{ee} = r_{hh}^*$ .

## 2.4 Application of the criterion

The most important observation is that after a unitary transformation to the so-called Majorana basis, by means of the matrix

$$\Omega = \sqrt{\frac{1}{2}} \begin{pmatrix} 1 & 1 \\ -i & i \end{pmatrix}, \quad (2.41)$$

one can write

$$\text{Det}(1 - r_N r_{NS}) = \text{Det}(1 + O_N r), \quad (2.42)$$

with  $O_N = -\Omega r_N \Omega^\dagger$  and  $r = \Omega r_{NS} \Omega^\dagger$ . It can now easily be shown that due to particle-hole symmetry both matrices  $O_N$  and  $r$  are real orthogonal matrices. For  $r$  we find for example that

$$\begin{aligned} r &= \frac{1}{2} \begin{pmatrix} 1 & 1 \\ -i & i \end{pmatrix} \begin{pmatrix} r_{ee} & r_{eh} \\ r_{eh}^* & r_{ee}^* \end{pmatrix} \begin{pmatrix} 1 & -i \\ 1 & i \end{pmatrix} \\ &= \begin{pmatrix} (r_{ee} + r_{ee}^*) + (r_{eh} + r_{eh}^*) & i(r_{ee} - r_{ee}^*) + i(r_{eh}^* - r_{eh}) \\ i(r_{ee}^* - r_{ee}) + i(r_{eh}^* - r_{eh}) & (r_{ee} + r_{ee}^*) - (r_{eh} + r_{eh}^*) \end{pmatrix} \end{aligned} \quad (2.43)$$

This matrix is obviously real and because it is unitary it is also orthogonal. Analogously one can show that  $O_N$  is real.

The number  $N$  of zero energy bound states is now equal to the multiplicity of the eigenvalue  $-1$  of  $O_N r$ . Since this is a real orthogonal matrix it can only have the eigenvalues  $1$ ,  $-1$  and pairs of  $e^{\pm i\varphi}$ . Therefore one has  $\text{Det}(O_N r) = (-1)^N$ . Furthermore equation (2.39) tells us that  $\text{Det}(r_N) = \text{Det}(O_n) = 1$  is real. This implies the parity of the number of Majorana fermions is encoded in the scattering matrix of the wire in the form  $\text{Det}(r) = (-1)^N$ . This provides the desired criterion. This method has the advantage that it does not rely on the system to be translationally invariant. Furthermore the step of calculating the determinant of the scattering matrix is simpler than calculating the pfaffian of a giant matrix. Finally one should emphasize again that only information about the zero energy scattering matrix is needed in order to calculate the topological number. This is an advantage compared to Kitaev's criterion which takes the full Hamiltonian as input.

## 2.4 Application of the criterion

We now apply this criterion to the wire system with non-uniform Zeeman field. We also applied it to a different geometry where the field of the solenoids all point in the same direction. In this second geometry the B-field does not resemble rotating behavior but has a spatially changing angle. To see how well this maps to a model of the form of equation (2.28), figure 2.3 (b) shows the magnitude of the B-field and the effective spin-orbit coupling. While for the first system of alternating field direction, the values vary only little around their average values, for the second system they have decisive drops where the field goes to zero and the effective spin-orbit coupling even changes sign briefly. For the first one would expect that the spatial structure of the parameters does not destroy the topological phase, but it is not entirely clear that this should also happen for the second system.

## 2 Majorana Fermions

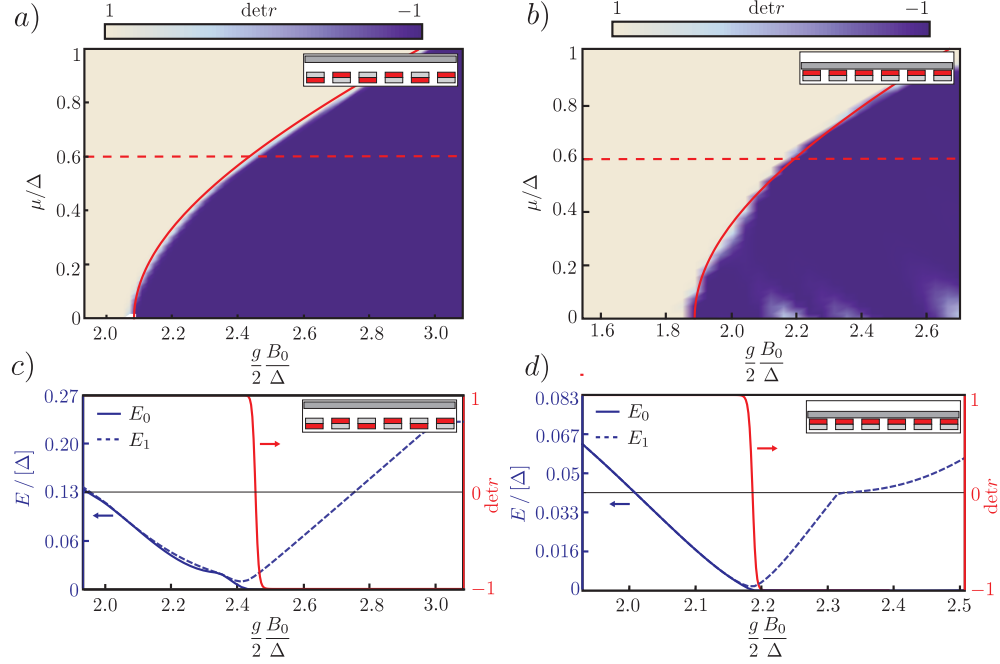


Figure 2.5: (a) Phase diagrams for both geometries of solenoid arrays. We are in the topological phase for  $\det(r) = -1$ . The solid red lines describe the phase transition according to (2.30) with an average B-field in the wire of  $0.48B_0$  in the first geometry and  $0.53B_0$  in the second geometry. (b) Cuts through the phase diagrams corresponding to the dashed red lines in (a). The cuts show the values of the two lowest lying positive energy solutions as a function of the field strength.

The scattering matrix for both systems were now calculated using the formula

$$S(0) = S_0 \frac{1 + i\pi\nu W^\dagger H^{-1}W}{1 - i\pi\nu W^\dagger H^{-1}W} S_0^T \quad (2.44)$$

from [1]. This describes the tunnel coupling of a lead via the coupling  $W$  to a wire described by  $H$ .  $\nu$  denotes the density of states of the leads and  $S_0 S_0^T$  is the scattering matrix for the lead in the absence of the tunnel coupling.

The phase diagrams for both cases were calculated and they both show a topological phase. Furthermore the Hamiltonians were diagonalized and the behavior of their lowest two positive eigenvalues was calculated across a cut through the topological phase transition. This situation is depicted in figure 2.5. One can clearly see how the lowest-lying energy level goes to zero across the transition and stays there, whereas the next eigenvalue takes finite values inside the topological phase.

It is interesting that the second geometry with parallel magnetic fields also exhibits a topological phase. A possible way to think about this is that the dips in the effective

spin-orbit coupling and in the magnitude of the B-field causes the system to locally leave the topological phase. This would cause bound states at the phase boundaries, but those would not be Majorana fermions because both boundaries are too close and Majorana fermions would immediately split up and form finite energy sub gap states. Therefore one might still have Majorana fermions together with several sub gap states that do not disturb the Majorana fermions at the ends but effectively lower the gap for the system. The fact that the second lowest energy eigenstate for this geometry seems to stay at a lower energy than the one from the other geometry is in favor of this possible explanation.

To sum up this section, we have shown how spatially varying Zeeman fields can be mapped to an effective spin-orbit interactions. In particular this can be used as a substitute for real spin-orbit interaction when one tries to build a topological superconductor. We have shown this topological phase for two sample systems. One where the effective spin-orbit coupling qualitatively resembles the Hamiltonian (2.28) with only slowly varying coefficients of Zeeman field strength and spin-orbit strength. In the other system we discussed both parameters were strongly position depended. Nevertheless a topological phase emerged, but we found that the band gap might be lower in this case. In both cases the phase transition can be qualitatively described by (2.30) for an effective constant field strength in the wire.

The geometries for both systems have an array of magnets in them, that creates a varying magnetic field. It should be noted that this is not the only way to create a varying Zeeman field. One could use a material with an anisotropic  $g$ -factor and bend the nanowire. In this geometry uniform magnetic field will then also cause a varying Zeeman field. This would allow for higher magnetic fields than in the other case.



### 3 Majorana qubits

In this section we will introduce qubits made of Majorana fermion and discuss which quantities are relevant to investigate their robustness. This includes a general discussion of the quantities that are of interest to qubit dephasing as well as setting this in relation to the properties special to Majorana qubits.

First of all let us briefly recall what a qubit is. A qubit is a system that takes values in a two-dimensional Hilbert space. For a given basis of this space labeled  $|0\rangle$  and  $|1\rangle$  the qubit can then take one of the infinite amount of states of the form

$$|\varphi\rangle = \alpha|0\rangle + \beta|1\rangle, \quad (3.1)$$

where  $|\alpha|^2 + |\beta|^2 = 1$ . This is in contrast to classical bits, which can only take the two values 0 and 1.

#### 3.1 Structure of the Majorana Qubits

When we consider a Majorana qubit we assume that we have four Majorana fermions  $\gamma_i$ ,  $i = 1 \dots 4$  all at zero energy. Formally those can be combined into two ordinary fermion of the form

$$\begin{aligned} c_1 &= \gamma_1 + i\gamma_2 \\ c_2 &= \gamma_3 + i\gamma_4. \end{aligned} \quad (3.2)$$

We can now use the eigenvalues of the corresponding number operators  $n_j = c_j^\dagger c_j$  to label the four degenerate ground states of our system. The eigenstates are simply  $|00\rangle$ ,  $|01\rangle$ ,  $|10\rangle$  and  $|11\rangle$ . The qubit is now formed by taking a subspace of definite parity. The advantage of defining a qubit like this over defining it as the space spanned by only one of the combined fermions, is that no particles have to be added or removed to flip the qubit (since only electron parity is conserved in a superconductor).

In order to theoretically work with this qubit it is very helpful to define Pauli matrices for our qubit in terms of the Majorana operators. One way to do that is as follows

$$\sigma_x = -i\gamma_2\gamma_3, \quad \sigma_y = i\gamma_1\gamma_3 \quad \text{and} \quad \sigma_z = -i\gamma_1\gamma_2. \quad (3.3)$$

One can check that these fulfill the desired commutation relations. One interesting thing to note is that  $\gamma_4$  does not appear. In fact one can in principle choose Pauli matrices in a way that any one of the Majorana fermions does not appear. The reason for this is, that by choosing the Pauli matrices we also specify which Majorana fermions we would use to make any actual measurement in an experiment. The Majorana fermion that does not appear in our Pauli matrices (and which we therefore would not use for any hypothetical

### 3 Majorana qubits

measurement) has the effect of changing the parity subspace, but conserving the qubit. In other words it is a unitary transformation from the even parity qubit to the odd parity qubit. All the Pauli matrices are unaffected by this because they commute with  $\gamma_4$ . Therefore if any perturbation couples to  $\gamma_4$  it will never effect the information stored in the qubit.

## 3.2 General Dephasing

One of the most important aspects of the state of a qubit is the relative phase between  $\alpha$  and  $\beta$  in equation (3.1). It is this information that gets most easily lost when the qubit is coupled to the environment. A very convenient way to investigate this is by means of density matrices. All the information about the state of a qubit is stored in its density matrix. This is a two-dimensional hermitian matrix with trace one. For a qubit the density matrix can generally be expressed in the form

$$\rho_q(t) = \frac{1}{2}\mathbb{I} + \mathbf{v}(t) \cdot \boldsymbol{\sigma}. \quad (3.4)$$

A further important aspect of density matrices is that they can also describe mixtures of different states. This is important because not knowing the phase difference between the coefficients of the qubit is formally the same as having a mixture between the states  $|0\rangle$  and  $|1\rangle$  at the ratio  $\alpha : \beta$ . The density matrix now provides an easy way to distinguish between a mixed state and a so-called pure state. Only for a pure state the density matrix can be written as  $\rho = |\varphi\rangle\langle\varphi|$  for some state  $|\varphi\rangle$ . It can be shown that  $\text{Tr}(\rho^2) \leq 1$  and that  $\text{Tr}(\rho^2) = 1$  if and only if the state is pure. From equation (3.4), and using the fact that the Pauli matrices are traceless and anti-commute with one another, we get

$$\text{Tr}(\rho_q(t)^2) = \frac{1}{2} + 2\mathbf{v}^2(t). \quad (3.5)$$

If we assume that our systems are initially prepared in pure states, this gives us a normalization condition on  $\mathbf{v}$  in equation (3.4), i.e.

$$|\mathbf{v}(0)|^2 = \frac{1}{4}. \quad (3.6)$$

This tells us that we simply need to find the time dependence of  $\mathbf{v}$  in order to get information about how pure our state is. In particular this is related to decoherence of the qubit. Which simply means the decay of the off-diagonal elements of the density matrix. Strictly speaking this only makes sense if some specific basis needs to be selected for a physical reason. If the basis in which  $\sigma_z$  is diagonal is the appropriate one for our system, then the off-diagonal elements of the density matrix are simply  $v_1(t) \pm iv_2(t)$ . This relates the off-diagonal elements to equation (3.5). Usually one candidate for the special basis we need to use is simply the eigenbasis of the qubit.

Pauli matrices are traceless and furthermore have the following multiplication properties

$$\sigma_j \sigma_k = \delta_{jk} + i \sum_l \varepsilon_{jkl} \sigma_l. \quad (3.7)$$

This implies the useful relation

$$\frac{1}{2}\text{Tr}(\sigma_j\sigma_k) = \delta_{jk} \quad (3.8)$$

With the help of equation (3.8) we can obtain the components of  $\mathbf{v}$  as

$$\begin{aligned} \langle\sigma_j\rangle(t) &= \frac{1}{2}\text{Tr}[\rho_q(t)\sigma_j] \\ &= \frac{1}{2}\text{Tr}\left[\left(\frac{1}{2}\mathbb{I} + \sum_k v_k(t)\sigma_k\right)\sigma_j\right] \\ &= v_j(t). \end{aligned} \quad (3.9)$$

We will now consider a bath coupled to our system. Initially the density matrix now takes the form

$$\rho(0) = \rho_q(0) \otimes \rho_B. \quad (3.10)$$

We can now find the reduced density matrix describing our qubit by tracing over the bath degrees of freedom. In particular we have

$$\rho_q(t) = \text{Tr}_B\rho(t), \quad (3.11)$$

Where  $\text{Tr}_B$  denotes the trace over the bath degrees of freedom. Let us now take an operator of the form

$$A = A_q \otimes \mathbb{I}, \quad (3.12)$$

that is an operator that only acts on our system and not on the bath. One can now show that

$$\text{Tr}(A\rho) = \text{Tr}_q(A_q\rho_q). \quad (3.13)$$

We can use the previous equations to find the expectation value of the Pauli matrices. This way we obtain

$$\begin{aligned} \text{Tr}_q(\rho_q(t)\sigma_j) &= \text{Tr}_q(\text{Tr}_B(U(t)(\rho_q(0) \otimes \rho_B)U^\dagger(t))\sigma_j) \\ &= \text{Tr}(U(t)(\rho_q(0) \otimes \rho_B)U^\dagger(t)(\sigma_j \otimes \mathbb{I})) \\ &= \text{Tr}((\rho_q(0) \otimes \rho_B)U^\dagger(t)(\sigma_j \otimes \mathbb{I})U(t)) \\ &= \text{Tr}((\mathbb{I} \otimes \rho_B)(\rho_q(0) \otimes \mathbb{I})U^\dagger(t)(\sigma_j \otimes \mathbb{I})U(t)) \\ &= \langle(\rho_q(0) \otimes \mathbb{I})U^\dagger(t)(\sigma_j \otimes \mathbb{I})U(t)\rangle \\ &= \frac{1}{2}\langle U^\dagger(t)(\sigma_j \otimes \mathbb{I})U \rangle + \sum_i v_i(0)\langle(\sigma_i \otimes \mathbb{I})U^\dagger(t) \\ &= \sum_i v_i(0)\langle(\sigma_i \otimes \mathbb{I})(\sigma_j \otimes \mathbb{I})(t)\rangle. \end{aligned} \quad (3.14)$$

This tells us that all the information about the reduced density matrix is contained in the set of  $\sigma$ - $\sigma$  correlation functions for the full system. We can now relate this to our Majorana fermions by means of (3.3), which means that the Majorana 4-point functions contain all the information about the qubit.

For the rest of the thesis we will only be concerned with expectation values. Therefore explicit tensor products and identity operators will be omitted.

### 3.3 Majorana 4-point functions

We will now look at the Majorana 4-point functions perturbatively. In order to do that we think of calculating a time-ordered spin correlation function and therefore a time-ordered Majorana 4-point function. We can then in principle obtain the non-time-ordered correlation function by choosing a definite sign for  $t$  and performing the ordering.

We assume that the Majorana fermions are not directly coupled in the unperturbed system. This means they all have energy zero. We would now like to classify the terms in their perturbative expansions with respect to the localized nature of the Majorana fermions. A general local perturbation that couples the Majorana fermions the bulk electronic states will have the form

$$H_I = i \sum_j \gamma_j \Gamma_j. \quad (3.15)$$

Here the Majorana fermions are coupled to  $\Gamma_k$  operators. We will show that those  $\Gamma_k$  operators contain information about the perturbation as well as information about the position of the Majorana fermion with the same index. We will now explain the form of the Hamiltonian in equation (3.15). We start by looking the expansion of an ordinary field operator in terms of the operators of the diagonalized system. This will take the form

$$\Psi(x) = \sum_j \alpha_j(x) \gamma_j + \sum_l \left[ \beta_{l+}(x) b_l^\dagger + \beta_{l-}(x) b_l \right], \quad (3.16)$$

where the  $\gamma$ s denote the Majorana fermion operators and the  $b$ s denote the operators that correspond to the other Bogoliubov quasi-particles. We will now determine the coefficients  $\alpha_k(x)$ . In order to do that we anti-commute equation (3.16) with  $\gamma_k$ . Because different Majorana fermions anti-commute and because the Majorana fermions also have to anti-commute with all the other Bogoliubov operators that diagonalize the system, we have

$$\{\Psi(x), \gamma_k\} = 2\alpha_k(x). \quad (3.17)$$

We can now use equation (2.4) to calculate (3.17) to obtain  $\alpha_j(x) = \frac{1}{2} f_j^*(x)$ . This means that the field operators can be expanded in the form

$$\Psi(x) = \sum_j \frac{f_j^*(x)}{2} \gamma_j + \dots, \quad (3.18)$$

where the dots correspond to terms that do not contain Majorana operators. This way we obtain the following expression for the density operator

$$\begin{aligned} \rho(x) &= \Psi^\dagger(x) \Psi(x) \\ &= \sum_j \frac{1}{2} \gamma_j \left( f_j(x) \Psi(x) - f_j^*(x) \Psi^\dagger(x) \right) + \dots, \end{aligned} \quad (3.19)$$

### 3.3 Majorana 4-point functions

where the dots correspond to terms that do not contain Majorana operators and therefore do not interest us to low orders in perturbation theory. We now define

$$\tilde{\rho}(x) = \sum_j \frac{1}{2} \gamma_j \left( f_j(x) \Psi(x) - f_j^*(x) \Psi^\dagger(x) \right) \quad (3.20)$$

which is the part of the density operator that involves coupling of the Majorana fermions to other electronic states. Strictly speaking it also involves coupling between different Majorana fermions at this point. In particular if we were to expand the rest of the field operators according to equation (3.16), we would get terms involving different pairs of Majorana fermions. If the different Majorana fermions are far enough apart, the terms which couple the Majorana fermions directly will be negligible. Therefore we will stick to a notation involving field operators, because it is easier to deal with them than with exact bulk eigenstates. With the help of this expression we can now extract the Majorana electron coupling from a local Hamiltonian like

$$\begin{aligned} H &= \int dx V(x) \rho(x) \\ &= i \sum_j \gamma_j \Gamma_j, \end{aligned} \quad (3.21)$$

by simply substituting  $\tilde{\rho}$  in the form of equation (3.20) for  $\rho$ . This gives us a Hamiltonian of the form (3.15) with

$$\Gamma_j = -i \frac{1}{2} \int dx \left( V(x) f_j(x) \Psi(x) - V(x) f_j^*(x) \Psi^\dagger(x) \right). \quad (3.22)$$

To simplify the notation we define  $g_j = \frac{1}{2} V f_j$ . The important thing to note here, is that the functions  $g_j$  are localized at the position of the Majorana fermion. Furthermore it is interesting to note that we have

$$\{\gamma_j, \Gamma_k\} = 0. \quad (3.23)$$

This deserves further elaboration.  $\gamma_j$  has to anti-commute with  $\Gamma_j$  which follows from the properties of the Majorana fermion and because the perturbation Hamiltonian has to be self-adjoint. For different indices equation (3.23) is only valid for Majorana fermions without overlap. With the definition of  $\Gamma_k$  we obtain

$$\begin{aligned} \{\gamma_j, \Gamma_k\} &= \int dx \left( g_k(x) \{\gamma_j, \Psi(x)\} - g_k^*(x) \{\gamma_j, \Psi^\dagger(x)\} \right) \\ &= \int dx \left( g_k(x) f_j(x) - g_k^*(x) f_j^*(x) \right) \\ &\approx 0, \end{aligned} \quad (3.24)$$

where the last line follows from the fact that  $g_k$  and  $f_j$  have negligible overlap because  $g_k$  is localized at the position of  $\gamma_k$ . This means, that the fact that the Majorana fermions are far apart causes the anti-commutator to vanish. It should be noted that the previous paragraph remains valid even if we assume the potential to be time dependent.

### 3 Majorana qubits

We would like to do a perturbative expansion of the correlation functions of the Majorana fermions, in particular of the Majorana 4-point functions. For a particular order of perturbation theory only those terms survive where each Majorana fermion appears an even number of times. This is the case because we can use Wick's theorem to pair up operators<sup>1</sup>. Only those pairings that contain the same Majorana fermions twice or no Majorana fermion at all, are not going to vanish. The reason for this is that we trace over the degenerate ground state and this trace vanishes for a single Majorana fermion. After pairing up all the Majorana fermions, only the non-trivial contribution from the correlation function of the  $\Gamma$ s remains. Here we have to make the important distinction between the correlation function of the same and different  $\Gamma$ s. Let us first write  $\Gamma_k$  in the form

$$\Gamma_k = -i \int dx \tilde{g}_k(x, t) \cdot \Psi(x, t), \quad (3.25)$$

where  $\Psi(x, t) = (\Psi(x, t), \Psi^\dagger(x, t))^T$  as earlier and we additionally introduced  $\tilde{g}_k(x, t) = (g_k(x, t), -g_k^*(x, t))^T$ . In order to shorten the notation we will use the common replacement  $(x, t) \rightarrow 1$ ,  $(x', t') \rightarrow 2$  etc. If we look at any type of correlation function of the  $\Gamma$ s, time-ordered for example, it takes the form

$$\begin{aligned} \langle T(\Gamma_j(t)\Gamma_k(t')) \rangle &= - \int dx dx' \langle T((\tilde{g}_j(1) \cdot \Psi(1))(\tilde{g}_k(2) \cdot \Psi(2))) \rangle \\ &= - \int dx dx' \left( \tilde{g}_j(1)^T \langle T\left(\begin{pmatrix} \Psi(1) \\ \Psi^\dagger(1) \end{pmatrix} \begin{pmatrix} \Psi(2) & \Psi^\dagger(2) \end{pmatrix}\right) \tilde{g}_k(2) \right) \\ &= - \int dx dx' \left( \tilde{g}_j(1)^T \tau_x \langle T\left(\begin{pmatrix} \Psi^\dagger(1) \\ \Psi(1) \end{pmatrix} \begin{pmatrix} \Psi(2) & \Psi^\dagger(2) \end{pmatrix}\right) \tilde{g}_k(2) \right) \\ &= - \int dx dx' (\tilde{g}_j(1)^T \tau_x G(1, 2) \tilde{g}_k(2)), \end{aligned} \quad (3.26)$$

where

$$G(1, 2) = \begin{pmatrix} \langle T(\Psi^\dagger(1)\Psi(2)) \rangle & \langle T(\Psi^\dagger(1)\Psi^\dagger(2)) \rangle \\ \langle T(\Psi(1)\Psi(2)) \rangle & \langle T(\Psi(1)\Psi^\dagger(2)) \rangle \end{pmatrix}. \quad (3.27)$$

Furthermore  $\tau_x$  is a Pauli matrix in particle-hole space. We argued earlier that the  $\tilde{g}_j$  are localized at the positions of the Majorana fermions. Therefore the major contribution to the integrals for the case of  $j = k$  comes from the values of the Green function with the spatial arguments being equal. On the other hand for  $i \neq j$  it depends on the values of the Green function for  $x' - x \approx L$ . It is important to note that this property of equation (3.26) does not depend on the specific form of the Bogoliubov spinor. A different spinor structure (for example one including spin) would change the structure of the  $\tilde{g}_k$ s, the form of  $G$  and additionally would cause a different matrix related to the particle hole symmetry of the new spinor to appear instead of  $\tau_x$  in equation (3.26). What remains is

<sup>1</sup>Wick's theorem applies to Majorana fermions, because it applies to the combined fermion (3.2) and those are related to the Majorana fermions by a linear transformation. Furthermore we have shown that the  $\Gamma$ s anti-commute with the  $\gamma$ s. This of course still requires calculating a correlation function where wicks theorem is applicable. Other correlation functions that have to be related to the on calculated afterwards.

the structure that two spinors that are associated with the position of particular Majorana fermions are connected by an electronic superconducting Green function. Effects that result from this kind of correlation function can therefore in principle be controlled and suppressed by increasing the distance between the Majorana fermions. If the Majorana fermions are far enough apart, we can assume that they only couple to independent baths. In those cases the Pauli matrix correlation functions simplify dramatically. For example

$$\begin{aligned}\langle\sigma_z\sigma_z(t)\rangle &= -\langle\gamma_1\gamma_2\gamma_1(t)\gamma_2(t)\rangle \\ &= +\langle\gamma_1\gamma_1(t)\rangle\langle\gamma_2\gamma_2(t)\rangle\end{aligned}\tag{3.28}$$

and

$$\begin{aligned}\langle\sigma_x\sigma_y(t)\rangle &= \langle\gamma_2\gamma_3\gamma_1(t)\gamma_3(t)\rangle \\ &= -\langle\gamma_2\rangle\langle\gamma_1(t)\rangle\langle\gamma_3\gamma_3(t)\rangle \\ &= 0\end{aligned}\tag{3.29}$$

where we used the assumption that different Majorana fermions are not correlated at all. The interesting thing to note about this is that for a perturbation of the form (3.15) there is no preferred basis for the qubit, because all the Pauli matrix correlators will decay. This tells us that the qubit will not only decohere, but will go to a completely mixed state with a density matrix that is one half the identity matrix. The situation is a little bit different if only one of the Majorana fermions from equation (3.3) is coupled to the environment. In that case we will have a preferred basis. If only  $\gamma_3$  appears in the interaction Hamiltonian (3.15) for example, we see from equation (3.28) that the  $\sigma_z$  correlation function is constant and therefore the eigenvectors of  $\sigma_z$  form a preferred basis. In this basis the diagonal elements of the density matrix of our qubit will not decay and we would have only dephasing. The physical reason behind this is easiest to understand for potential perturbations (possibly time dependent). Different potential landscapes have different Majorana solutions. Therefore we get decay of the correlation function because the overlap of the Majorana wavefunctions is less than one. One can get rid of this form of decay if one looks at the correlation of instantaneous Majorana fermions. In this case fast changes in the potential will cause a mixing of the instantaneous Majorana fermion and bulk states, which also causes information to get lost. Quantum noise, in particular phonons may also have a similar effect.

### 3.4 Topological protection

We mentioned earlier, that Majorana fermion appear in so-called topological phases and that they are supposed to have some sort of robustness against perturbations. This robustness is often called topological protection. But now the question is what is exactly meant by topological protection and to what a degree can it be quantified. We will now state how we quantify topological protection and then argue why it is helpful to think about it this way.

Under topological protection we understand how the quantities of interest (mostly Majorana correlation functions) depend on the separation between the Majorana fermions,

### 3 Majorana qubits

in particular how fast it decreases with respect to the separation. This definition is motivated by several aspects. First of all the fascinating thing about the topological phase is, that we have those spatially well separated Majorana fermions describing a single fermionic state. In the limit of having a semi-infinite geometry where there is only one Majorana fermion present, no perturbation can ever remove it. This tells us that the protection of Majorana fermions becomes perfect for infinite separations and the question remains of how fast it gets there. On the other hand the correlation functions of a single Majorana fermion with itself are never influenced by the separation of the Majorana fermions (assuming it is always large enough such that they do not have any overlap). Yet these correlation function can still have significant influence on the qubit as can be seen from equation (3.28). Since this involves virtual transitions to other electronic states it is protected by the energy gap with respect to those other states. Those states might be the bulk state of the superconducting wire itself, or lower lying states from a lead that was brought there on purpose. We did not include the energy gap in this classification of topological protection, because even though it protects the system against certain couplings it is not unique to the topological phase. Or to put it another way, it would appear the same way for a topologically trivial superconductor with some non-Majorana mid-gap state. Another reason, from the context of quantum computation, is that braiding needs to be done adiabatically, which means on timescales longer than the timescale set by the energy gap. In this context protection on the timescales shorter than the timescale associated with the gap might not be very helpful.

We will now phrase the above discussion in terms of correlation functions. If we have two Majorana fermions  $\gamma_1$  and  $\gamma_2$  at a distance  $L$  apart then the topological protection is how the correlation function  $\langle \gamma_1(t)\gamma_2 \rangle$  decays with  $L$ . To put it into the language of the previous paragraph, the correlation function of  $\Gamma$ s for different indices are protected while the ones for the same index are not. This also tells us that the correlation functions of different Pauli matrices are always protected, because they have to couple two different Majorana fermions, which results in at least one correlation function of different  $\Gamma$ s. On the other hand the correlation of the same Pauli matrix at different times is never entirely protected in our sense, because it always contains  $L$  independent contribution that do not come from coupling different Majorana fermions.

## 4 Perturbative corrections

In this section we will classify and discuss the different corrections to the Majorana Green functions and give some explicit examples for when each type of correction may arise. As discussed earlier, we mainly distinguish two types of corrections. The topologically protected ones, that is the ones that can be eliminated by letting the distance between the Majorana fermions go to infinity, and the local ones, that only couple to a single Majorana fermion.

### 4.1 Local perturbations

These involve all corrections that do not couple the Majorana fermions to each other. This means that they do not introduce any direct coupling between the Majorana fermions, and it also means that if the perturbation couples the Majorana fermions to baths, then the baths for the individual Majorana fermions are independent of one another. A very general account of how those kind of perturbations influence the  $\gamma_1 - \gamma_1$  correlation functions is given in Goldsteins and Chamons paper [6]. Their treatment includes boson-mediated coupling to electron baths as well as classical noise of various kinds. There is however an important other type of corrections that occurs in this situation, namely non-adiabatic corrections in the case of time dependent classical potentials. This might occur for instance when one wants to change the position of the Majorana fermions, by moving the domain wall to which they are pinned. It should also be considered in the case of noise, since the noise may have to some extent only the effect of moving the Majorana fermion around or changing its shape. A detailed study of the non-adiabatic corrections to braiding of Majorana fermions in a two-dimensional topological superconductor can be found in [3]. Here we will only be concerned with the effect on a single Majorana fermion and not with braiding. We will now derive the non-adiabatic corrections and then apply them to classical noise in order to compare to the non-adiabatic treatment of Goldstein and Chamon. Furthermore we will apply it to the simple example of a moving Majorana fermion.

We want to calculate the correlation function of instantaneous Majorana fermions. First of all let us specify what we mean by that. We look at our wire system, described by some time independent Hamiltonian  $H_0$ , together with some time and space dependent potential

$$V(t) = \int dx V(x, t) \Psi^\dagger(x) \Psi(x). \quad (4.1)$$

This potential may describe our moving domain wall or noise fluctuations.

We now look at the set of instantaneous eigenstates of our system. We denote them

#### 4 Perturbative corrections

with  $|\gamma(t)\rangle$ ,  $|\gamma'(t)\rangle$ ,  $|b_{k+}\rangle$  and  $|b_{k-}\rangle$ . They fulfill the equations

$$\begin{aligned} (H_0 + V(t))|\gamma(t)\rangle &= 0 \\ (H_0 + V(t))|\gamma'(t)\rangle &= 0 \\ (H_0 + V(t))|b_{k\pm}(t)\rangle &= \pm E_k |b_{k\pm}\rangle. \end{aligned} \quad (4.2)$$

This assumes that at each time  $t$  we still have two zero modes pinned to two different domain walls. We now try to find the time evolution of the state

$$|\Gamma(t)\rangle = a_0(t)|\gamma(t)\rangle + \sum_k \left( a_k(t)e^{i\Theta_k(t)}|b_{k-}(t)\rangle + a_k^*(t)e^{-i\Theta_k(t)}|b_{k+}(t)\rangle \right), \quad (4.3)$$

under the initial conditions  $a_0 = 1$  and  $a_k = 0$  for all  $k$ . Furthermore  $\Theta_k(t)$  denotes the accumulated dynamical phase of the bulk states, i.e.

$$\Theta_k = \int_0^t E_k(t') dt'. \quad (4.4)$$

Notice that we did not include a second Majorana fermion  $\gamma'(t)$  in equation (4.3) nor did we include a third and fourth one. The reason for this is, that we assume that the system is large enough and only one of the Majorana fermions is subject to the potential.

We can now easily specify what we mean by the time correlation of an instantaneous Majorana fermion with itself. We mean the factor  $a_0$  in equation (4.3). This factor tells us precisely how much of the original Majorana fermion is still present at later times in terms of a potentially deformed and shifted instantaneous Majorana fermion.

##### 4.1.1 Calculation of the correlation function

Now in order to calculate the time dependence of  $a_0$  we use a standard procedure to calculate non-adiabatic corrections. We plug equation (4.3) into the Schrödinger equation. For this purpose we first compute the time derivative of equation (4.3). We obtain

$$\begin{aligned} \partial_t |\Gamma(t)\rangle &= \dot{a}_0(t)|\gamma(t)\rangle + \sum_k \left( \dot{a}_k(t)e^{i\Theta_k(t)}|b_{k-}(t)\rangle + \dot{a}_k^*(t)e^{-i\Theta_k(t)}|b_{k+}(t)\rangle \right) \\ &+ a_0(t)|\dot{\gamma}(t)\rangle + \sum_k \left( a_k(t)e^{i\Theta_k(t)}|\dot{b}_{k-}(t)\rangle + a_k^*(t)e^{-i\Theta_k(t)}|\dot{b}_{k+}(t)\rangle \right) \\ &+ \sum_k iE_k(t) \left( a_k(t)e^{i\Theta_k(t)}|b_{k-}(t)\rangle - a_k^*(t)e^{-i\Theta_k(t)}|b_{k+}(t)\rangle \right). \end{aligned} \quad (4.5)$$

With the help of equation (4.2) we see that the last line of equation (4.5) gets exactly canceled by the other side of the Schrödinger equation. This means that for the Schrödinger equation to be true, the first two lines of equation (4.5) have to add to zero, that is

$$\begin{aligned} \dot{a}_0(t)|\gamma(t)\rangle + \sum_k \left( \dot{a}_k(t)e^{i\Theta_k(t)}|b_{k-}(t)\rangle + \dot{a}_k^*(t)e^{-i\Theta_k(t)}|b_{k+}(t)\rangle \right) &= \\ -a_0(t)|\dot{\gamma}(t)\rangle - \sum_k \left( a_k(t)e^{i\Theta_k(t)}|\dot{b}_{k-}(t)\rangle + a_k^*(t)e^{-i\Theta_k(t)}|\dot{b}_{k+}(t)\rangle \right). \end{aligned} \quad (4.6)$$

We can now project out individual parts of equation (4.6). First of all let us project out the  $|\gamma(t)\rangle$  part. We obtain

$$\dot{a}_0(t) = -\frac{1}{2} \sum_k \left( a_k(t) e^{i\Theta_k(t)} \langle \gamma(t) | \dot{b}_{k-}(t) \rangle + a_k^*(t) e^{-i\Theta_k(t)} \langle \gamma(t) | \dot{b}_{k+}(t) \rangle \right). \quad (4.7)$$

The  $\langle \gamma(t) | \dot{\gamma}(t) \rangle$  term on the right hand side vanished because  $\langle \gamma(t) | \gamma(t) \rangle = 2$ . In order to replace the expressions of the form  $\langle \gamma(t) | \dot{b}_{k+} \rangle$  we employ the standard trick to differentiate the last line of equation (4.2) with respect to time and then multiply it with  $|\gamma(t)\rangle$  from the left. For brevity we suppress the time argument of the bras and kets. This way we obtain the following equations

$$\begin{aligned} \langle \gamma | \dot{b}_{k+} \rangle &= \frac{\langle \gamma | \dot{V}(t) | b_{k+} \rangle}{E_k(t)} \\ \langle \gamma | \dot{b}_{k-} \rangle &= -\frac{\langle \gamma | \dot{V}(t) | b_{k-} \rangle}{E_k(t)}. \end{aligned} \quad (4.8)$$

If we plug this into equation (4.7) we obtain

$$\dot{a}_0(t) = -\frac{1}{2} \sum_k \left( -a_k(t) e^{i\Theta_k(t)} \frac{\langle \gamma | \dot{V}(t) | b_{k-} \rangle}{E_k(t)} + a_k^*(t) e^{-i\Theta_k(t)} \frac{\langle \gamma | \dot{V}(t) | b_{k+} \rangle}{E_k(t)} \right). \quad (4.9)$$

This equation alone is not enough to solve for  $a_0$ . We can obtain the remaining equation that we need by simply projecting out the  $|b_{k-}(t)\rangle$  part of equation (4.6). This way we obtain the equations

$$\dot{a}_k(t) e^{i\Theta_k(t)} = -a_0(t) \langle b_{k-} | \dot{\gamma} \rangle + \dots \quad (4.10)$$

Here the dots stand for terms that also come with a  $a_k$  or  $a_k^*$ . Since we will try to get an approximate solution iteratively in  $a_k$  and  $a_0$  to lowest non-vanishing order, those terms are not going to be important to us. This way we also avoid to deal with Berry phases that might appear for degenerate bulk states. We use the simple relation  $\langle b_{k-} | \dot{\gamma} \rangle = -\langle \dot{b}_{k-} | \gamma \rangle$  together with equation (4.8) to simplify equation (4.10). We also drop the higher order terms completely and set  $a_0$  to its initial value. This way we obtain

$$\dot{a}_k(t) \approx -e^{-i\Theta_k(t)} \frac{\langle b_{k-} | \dot{V}(t) | \gamma \rangle}{E_k(t)}. \quad (4.11)$$

Analogously one finds the following expression for  $a_k^*$

$$\dot{a}_k^*(t) \approx +e^{i\Theta_k(t)} \frac{\langle b_{k+} | \dot{V}(t) | \gamma \rangle}{E_k(t)}. \quad (4.12)$$

These equations can now be integrated and plugged into equation (4.9), which can be solved afterwards.

Before we explicitly do that a few remarks on the relationship between  $\langle b_{k-} | \dot{V}(t) | \gamma \rangle$  and  $\langle b_{k+} | \dot{V}(t) | \gamma \rangle$  are in order. The easiest way to see this relation is to briefly go back

#### 4 Perturbative corrections

to second quantisation using equation (2.13). In second quantisation those two matrix elements can be written as  $\{b_k^\dagger, [V(t), \gamma]\}$  and  $\{b_k, [V(t), \gamma]\}$  respectively. Written this way it is obvious that one is the negative complex conjugate of the other. This is also consistent with the fact that equation (4.11) and equation (4.12) should be the complex conjugate to each other. Instead of referring back to second quantisation one could also employ the particle-hole symmetry operator in bra ket notation. This is a bit more tricky because the particle-hole symmetry operator is anti-linear and bra ket notation is only intuitive for linear operators. After those final remarks we can now state the approximate solution for  $a_0$ , which we have re-exponentiated. We have

$$a_0(t) \approx \exp \left( - \sum_k \left| \int_0^t dt' e^{-i\Theta_k(t')} \frac{\langle \gamma(t') | \dot{V}(t') | b_{k+}(t') \rangle}{E_k(t')} \right|^2 \right). \quad (4.13)$$

##### 4.1.2 Non-adiabatic effects of noise

We would now like to compare this to Goldsteins and Chamons result for the ordinary correlation function of Majorana fermions subject to noise. They found

$$\langle \gamma_{\text{na}}(t) \gamma_{\text{na}}(0) \rangle \approx \exp \left\langle \left( - \sum_k \left| \int_0^t dt' e^{-iE_k t'} \langle \gamma | V(t') | b_{k+} \rangle \right|^2 \right) \right\rangle. \quad (4.14)$$

Here the subscript on the  $\gamma$ s stands for non-adiabatic. Furthermore the  $\langle \dots \rangle$  denotes an ensemble average over the potential  $V$ . We assume that the  $V$  obey a Gaussian distribution and that their correlation function is translation invariant in time. Furthermore we assume that  $V$  fluctuates independently in space and time such that its correlation function factors like

$$\begin{aligned} \langle V(x_1, t_1) V(x_2, t_2) \rangle &= G(x_1 - x_2, t_1 - t_2) \\ &= G_X(x_1 - x_2) G_T(t_1 - t_2). \end{aligned} \quad (4.15)$$

Our result will differ only in terms of the integral in the exponent. We it is therefore enough to only compare the averaged squares of the integrals in the exponent. We define  $M_k = \langle \gamma | V(t') | b_{k+} \rangle$  as well as  $G_{M_k}(t' - t'') = \langle M_k(t') M_k^*(t'') \rangle$ . Here  $G_{M_k}$  only depends on time differences because the correlation function for the  $V$ s only depends on time differences and taking the matrix element of  $V$  only involves spatial integrations. We now obtain

$$\begin{aligned} \left\langle \left| \int_0^t dt' e^{-iE_k t'} \langle \gamma | V(t') | b_{k+} \rangle \right|^2 \right\rangle &= \int_0^t dt' \int_0^t dt'' e^{-iE_k(t'-t'')} G_{M_k}(t' - t'') \\ &= t \int_{-t}^t d\tau e^{-iE_k \tau} G_{M_k}(\tau) \end{aligned} \quad (4.16)$$

We would like to compare (4.16) to our result. In order to do that we approximate our result to lowest order in  $V(t)$ . This essentially means that we neglect the time

dependencies of the energies and of the states. Our result will therefore not capture the long time behavior of the instantaneous Majorana fermions anymore, because their wavefunctions at later times may differ significantly from their wavefunctions at the initial time. Nevertheless we can look for differences between our result and the one from Goldstein and Chamon at short times. Under these approximations and after performing an ensemble average our result takes the form

$$a_0(t) \approx \exp \left\langle \left( - \sum_k \left| \int_0^t dt' e^{-iE_k t'} \frac{\langle \gamma | \dot{V}(t') | b_{k+} \rangle}{E_k} \right|^2 \right) \right\rangle. \quad (4.17)$$

Here it is again written in an exponentiated way because we only expect small corrections. We can now rewrite this in the same way as equation (4.16) and obtain

$$\begin{aligned} \left\langle \left| \int_0^t dt' e^{-iE_k t'} \frac{\langle \gamma | \dot{V}(t') | b_{k+} \rangle}{E_k} \right|^2 \right\rangle &= \int_0^t dt' \int_0^t dt'' e^{-iE_k(t'-t'')} \frac{\partial_{t'} \partial_{t''} G_{M_k}(t' - t'')}{E_k^2} \\ &= -t \int_{-t}^t d\tau e^{-iE_k \tau} \frac{\ddot{G}_{M_k}(\tau)}{E_k^2}. \end{aligned} \quad (4.18)$$

For times big enough such that  $G_{M_k}$  and its derivatives are negligible, we can partially integrate equation (4.18) and discard the boundary terms. This way we obtain precisely equation (4.16). In other words, our approximations for equation (4.13) do not allow us to capture adiabatic behavior on large time scales. On the other hand let us look at small times, smaller than the time  $\tau_c$  it takes for  $G_{M_k}$  to fall to half its maximum. We assume  $t \ll E_k$ . This way we can approximate  $e^{-iE_k \tau}$  as one and furthermore expand  $G_{M_k}$  to quadratic order around its value at 0. This takes the form

$$G_{M_k}(\tau) \approx a - \frac{b}{2} \tau^2 \quad (4.19)$$

The approximation is illustrated in figure 4.1. Under these approximations equation (4.16) yields to lowest order in  $t$

$$\left\langle \left| \int_0^t dt' e^{-iE_k t'} \langle \gamma | V(t') | b_{k+} \rangle \right|^2 \right\rangle \approx 2at^2, \quad (4.20)$$

whereas our equation (4.18) yields

$$\left\langle \left| \int_0^t dt' e^{-iE_k t'} \frac{\langle \gamma | \dot{V}(t') | b_{k+} \rangle}{E_k} \right|^2 \right\rangle \approx 2b \frac{t^2}{E_k^2}. \quad (4.21)$$

If we additionally approximate  $\tau_c$  to be the time it takes for our expanded  $G_{M_k}$  to fall to half its value at  $\tau = 0$ , we obtain the relationship

$$b = \frac{a}{\tau_c^2}. \quad (4.22)$$

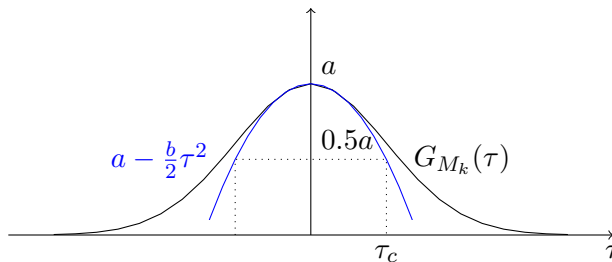


Figure 4.1: This illustrates the quadratic approximation  $G_{M_k}$  around its maximum. This approximation is furthermore used to determine the time  $\tau_c$  where  $G_{M_k}$  has fallen to half its value.

This relation is rather close to the exact result that we would get if we assumed a Gaussian of the form  $G_{M_k}(\tau) = aE^{-(b/2a)\tau^2}$ , which has (4.19) as an expansion. This would modify the right hand side of equation (4.22) by a constant factor of  $2 \ln 2$ . Therefore the approximate result qualitatively gives the right picture. We can use (4.22) to write equation (4.21) in the form

$$\left\langle \left| \int_0^t dt' e^{-iE_k t'} \frac{\langle \gamma | \dot{V}(t') | b_{k+} \rangle}{E_k} \right|^2 \right\rangle = 2a \frac{t^2}{(E_k \tau_c)^2}. \quad (4.23)$$

If we compare this to equation (4.20) we find that it differs by a factor of  $\frac{1}{(E_k \tau_c)^2}$ . In the adiabatic regime where we have  $E_k \tau_c > 1$  our result therefore yields less decay, as it should.

#### 4.1.3 Uniform movement of the Majorana fermion

In this section we would like to apply the result (4.13) to the uniform motion of a Majorana fermion. There are several reasons why one would like to move Majorana fermions around. One might want to braid them or bring them close together in order to create a splitting that one can measure. Even though we do not intend to generate a splitting the Majoranas have to be moved in either case. A suitable geometry for this might be the one introduced by Alicea et al. [2]. In addition to intentional movement of Majorana fermions, one might also have an unintentional drift.

We assume that the system is large enough such that its energy levels do not change as we move the Majorana fermion. This means that  $E_k(t) = E_k$  and  $\Theta(t) = E_k t$ . Furthermore the potential  $V$  takes the form

$$V(x, t) = \Theta(t) (V_0(x - vt) - V_0(x)). \quad (4.24)$$

Here  $V_0$  describes the potential of the domain wall, where the Majorana fermion sits. For its derivative we obtain

$$\dot{V}(x, t) = -v\Theta(t) = \partial_x V_0(x - vt). \quad (4.25)$$

Since the instantaneous eigenstates at each time are the ones at zero replaced by  $vt$  and  $\dot{V}$  moves in exactly the same way, we expect the matrix elements of  $\dot{V}$  as they appear in (4.13) to be time independent. Furthermore if we assume that the domain wall is rather steep, we can approximate  $\partial_x V(x) = h\delta(x)$ , where  $h$  is the height of the potential difference at the domain wall. The matrix element now simply samples the Majorana and bulk wavefunctions at the center of domain wall. Therefore the prefactor of the wavefunctions are important. In particular the bulk solutions have a prefactor that behaves as  $V^{-1/2}$ , where  $V$  is the volume of the system. The Majorana wavefunction has a prefactor of  $\xi^{-1/2}$ , where  $\xi$  is its localization length. This yields

$$\langle \gamma(t') | \dot{V}(t') | b_{k+}(t') \rangle = \frac{-vh}{\sqrt{\xi V}} s_k. \quad (4.26)$$

Here  $s_k$  is a dimensionless constant. Putting all this together we obtain

$$a_0(t) \approx \exp \left( - \sum_k \frac{h^2 v^2}{E_k^4 \xi^2} \frac{\xi}{V} |s_k|^2 (2 - 2 \cos(E_k t)) \right). \quad (4.27)$$

We can now argue that for long times, the cosine terms, are going to average out because we sum over many such terms with different frequencies. We therefore obtain

$$\begin{aligned} a_0(t) &\approx \exp \left( - \frac{2}{V} \sum_k \frac{h^2 v^2}{E_k^4 \xi^2} \xi |s_k|^2 \right) \\ &= \exp \left( - \frac{2}{V} \sum_k \frac{h^2 \Delta^2 v^2}{E_k^4 v_f^2} \xi |s_k|^2 \right) \end{aligned} \quad (4.28)$$

Where we replaced  $\xi = \frac{v_f}{\Delta}$  at one point. Here  $v_f$  is the Fermi velocity and  $\Delta$  the band gap of the system.

The result gives us a constant time-independent decay. When interpreting this result one should note that it is independent of the system size (as it should be) since the momentum sum scales as volume. A crucial role for the size of the decay is the speed with which one moves the domain wall with respect to the Fermi velocity. This suggests that it is beneficial to have high electron densities in order to have high Fermi velocities. Because the Fermi velocity is proportional to  $\xi$  this suggests an interpretation that an increase in  $\xi$  causes less decay. One can imagine that after moving the Majorana fermion a short distance, a less localized Majorana fermion will have more overlap with its former version at the old position. This then causes it to decay less. It is therefore good to have the localization length as large as possible with respect to the Fermi velocity as long as one does not cause overlap between different Majorana fermions. This discussion does not apply to the functional dependence of  $\xi$  on  $\Delta$ . There is no advantage connected to decreasing the size of the gap in order to increase the spread of the Majorana fermion. As for general adiabatic processes we have the bigger the gap the more adiabatic the process. In our case this is represented by the remaining  $\xi$  in equation (4.28) which goes as  $\frac{1}{\Delta}$ . We will now argue that the remaining terms in equation (4.28) do not play such an

## 4 Perturbative corrections

important role. First of all we can split a term of the form  $\Delta^2/E_k^2$ . For many different  $k$  this term will be of order unity and not have a significant effect. The remaining term is now  $\frac{h^2}{E_k}$ . For concreteness let us think of  $h$  as describing a step in  $\mu$  for the Hamiltonian (2.28) described earlier. This tells us that the gap of the system closes for a value of the chemical potential somewhere between  $\mu$  and  $\mu + h$ . For values of  $\mu$  close to the critical value of  $\mu$  the gap of the system is going to be given by the energy at  $p = 0$ . For small deviations from the critical value of  $\mu$  the band gap will therefore be proportional to those deviations and therefore proportional to  $h$ . From equation (2.31) we can calculate the proportionality factor as the derivative with respect to  $\mu$  at the critical value. This way we obtain  $\Delta \approx \frac{3\sqrt{B^2 - \Delta_s^2}}{B} h$ . Here  $\Delta_s$  is the bulk  $s$ -wave gap, not to be confused with the gap  $\Delta$  of the wire. We see that the prefactor is of order unity or smaller. Consequently  $\frac{h^2}{E_k}$  will be of order unity or bigger for several values of  $k$ . For larger values of  $h$  the band gap will not be given by the behavior of the spectrum close to zero anymore, but by some finite  $k$  minimum of the band which is lower than the  $k = 0$  one. This suggests that in that case  $h$  will also be of order of the gap or bigger.

## 4.2 Coupling between Majorana fermions

In this section we want to investigate how perturbations couple different Majorana fermions. The first thing to remark is, that any direct coupling between the Majorana fermions is going to be exponentially suppressed, because of the exponentially small overlap of the Majorana fermions. The question that now remains, is whether a bath can mediate interaction between the Majorana fermions. We have in particular the conducting states of the topological superconductor in mind.

### 4.2.1 Static perturbation

As a first very, simple example we are going to look at the splitting induced from a static potential perturbations. The result will not be very interesting in itself because it is generally believed that static perturbations will not easily drive the system out of the topological phase and therefore not destroy the Majorana fermions. This is also what we will find, but it is nice to have a direct check of this. Furthermore it gives us the opportunity to use our classification for topological protection on a very simple example.

Because we assumed that direct coupling is exponentially suppressed we need a perturbation close to each Majorana fermion to couple it to the bulk states. The bulk states may then mediate a splitting. The situation is depicted in figure 4.2 We expect that the Majorana nature of the states is not altered by this, but we will explicitly calculate the splitting to second order. In order to do that we will first use Lödwin partitioning to incorporate the effect of the perturbation to second order in our degenerate ground states. We will then obtain an effective perturbation for our degenerate ground state and analyze it. For this calculation we will again employ the first quantized picture.

We know that the Majorana states do not behave as ordinary states, because their expectation value for any operator is zero, as we know from equation (2.14). Furthermore

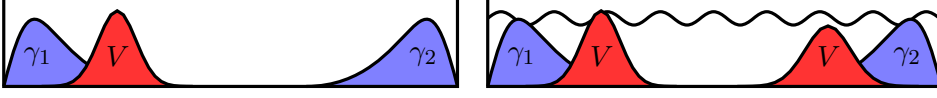


Figure 4.2: The left graphic illustrates how a static potential will not couple Majorana fermions directly due to their exponential small overlap. The right graphic illustrates the second order effect where a potential close to each individual Majorana fermion couples it to the bulk, which therefore might mediate a splitting.

we can use equation (2.13) together with an explicit form for the Majoranas (2.4) to get the formula

$$\begin{aligned} \langle \gamma_j | V | \gamma_k \rangle &= \int dx (f_j^*(x) f_k(x) V(x) - f_j(x) f_k^*(x) V(x)) \\ &\approx 0. \end{aligned} \quad (4.29)$$

This is the first quantized form of the fact that Majorana fermions are not directly coupled by local potentials due to their localization and separation.

The same way Majorana operators can be combined into ordinary fermionic operators, any two Majorana states can be combined into ordinary states of the form

$$\begin{aligned} |jk+\rangle &= |\gamma_j\rangle + i|\gamma_k\rangle \\ |jk-\rangle &= |\gamma_j\rangle - i|\gamma_k\rangle. \end{aligned} \quad (4.30)$$

This state has also zero energy and the important thing to notice is that we have

$$\begin{aligned} \langle jk+ | A | jk+\rangle &= \langle \gamma_j | A | \gamma_j \rangle + \langle \gamma_k | A | \gamma_k \rangle + i2\Im \langle \gamma_j | A | \gamma_k \rangle \\ &= +i2\langle \gamma_j | A | \gamma_k \rangle, \end{aligned} \quad (4.31)$$

where we used the properties (2.14) and (2.15). This tells that we can simply look at matrix elements of ordinary states and still obtain all the information about Majorana states. The reason to do that is simply that some arithmetic steps may seem more obvious in the ordinary state picture than in the Majorana state picture. Furthermore it is clear that we can also express matrix elements between ordinary states that are made up out of different Majorana fermions, as a linear combination of Majorana fermion matrix elements. For local operators where the matrix elements between different Majorana fermions are exponentially small, the matrix elements between ordinary states that are combined out of Majorana fermions are therefore also exponentially small.

Because we deal with degenerate states and the degeneracy is not lifted to first order in perturbation theory, we will employ Lödwin partitioning to perturbatively investigate the effect of a static potential. The idea behind Lödwin partitioning is to make a unitary

#### 4 Perturbative corrections

transformation that brings the Hamiltonian into a block diagonal form to a given order in the perturbation. One of the blocks then describes our degenerate subsystem and the other one the rest of the system. This means that we included the effects of the rest of the system on our subsystem to a given order in the perturbation by the means of Lödwin partitioning. After that we can then solve for the eigenvalues of the degenerate subsystem. The idea was first introduced by Per-Olov Lödwin [10]. A summary of it can be found in a book by Winkler [13].

Lödwin partitioning tells us that to second order the effective potential describing the effect of the perturbation on the degenerate states  $m$  (in our case the states generated by the Majorana fermions) due to coupling to the states  $l$  (in our case the gapped bulk states) is given by

$$\begin{aligned} V_{\text{eff},m,m'} &= V_{m,m'} + \frac{1}{2} \sum_l V_{m,l} V_{l,m'} \left[ \frac{1}{E_m - E_l} + \frac{1}{E_{m'} - E_l} \right] \\ &= - \sum_l V_{m,l} V_{l,m'} \frac{1}{E_l}. \end{aligned} \quad (4.32)$$

The first line gives the general equation and in the second line we simplified the expression by setting the energies of our subspace to zero and neglecting the first term since we already know that it comes from direct overlap between Majorana fermions and is exponentially small. We now take the expectation value of the effective potential with respect to a state  $m$  that is made up out of two Majorana states as described above. The expectation can now be approximated rather crudely by

$$|V_{\text{eff},m,m}| = \left| \sum_l V_{m,l} V_{l,m} \frac{1}{E_l} \right| < \frac{1}{\Delta} \sum_l V_{m,l} V_{l,m}, \quad (4.33)$$

where  $\Delta$  is the energy gap, such that  $\Delta \leq |E_l|$ . The crudeness of this estimate lies in using positive upper bounds for negative terms. We can now use the resolution of the identity in the following form

$$1 = \sum_l |l\rangle\langle l| + \sum_{m'} |m'\rangle\langle m'|, \quad (4.34)$$

where again  $l$  denotes bulk states and  $m'$  denotes ordinary states in the degenerate subspace of our Majorana states. If we solve that for the  $l$  sum and plug it into equation (4.33) we obtain

$$|V_{\text{eff},m,m}| < \frac{1}{\Delta} \left( (V^2)_{m,m} + \sum_{m'} V_{m,m'} V_{m',m} \right). \quad (4.35)$$

We already established that  $V_{m,m'}$  is exponentially small in  $\xi/L$  because  $V$  is a local operator. Furthermore the same applies to  $(V^2)_{m,m}$  since  $V^2$  is also a local potential perturbation.

We can now choose  $|m\rangle = |\gamma_i\rangle + i|\gamma_j\rangle$ . Then equation (4.35) and (4.31) tell us that the matrix elements between our Majorana fermions are exponentially small in  $\xi/L$ .

Because our degenerate ground state is always finite-dimensional, it also follows that upon diagonalizing our effective potential the biggest eigenvalue will also be exponentially small in the distance  $\xi/L$ . The topological protection against static perturbations can therefore be classified as exponential on the scale of the Majorana localization length  $\xi$ .

### 4.3 Phonon mediated coupling

The goal of this subsection is to estimate the splitting of Majorana fermions due to electron-phonon interaction. In order to do that we will try to calculate the Matsubara self-energy at low frequencies for the Majorana correlation function  $\langle T(\gamma_1(\tau_1)\gamma_2(\tau_2)) \rangle$ . In particular we are interested how the self-energy depends on the distance  $L$  between the Majorana fermions. The rate with which this correlation function goes to zero as a function of  $L$  will tell us how much the Majorana fermions are protected against the corresponding perturbation (according to our classification). In particular we would like to know whether it is also exponentially small in  $L$ , as in the static case, or not. We will start by relating  $\langle T(\gamma_1(t_1)\gamma_2(\tau_2)) \rangle$  to the self-energy of our Majorana fermions, before we actually calculate it.

#### 4.3.1 Split Majorana Green function

We would now like to have a look at how the self-energy may cause a splitting of the Majorana fermions in the simplest possible case. We take two Majorana fermions at zero energy together with a perturbation of the form  $V = i\frac{V_0}{2}\gamma_1\gamma_2$ . Of course this could be solved exactly to yield an energy splitting of  $V_0$ . This suggest that if we treat the problem perturbatively the self-energy we obtain should correspond to a splitting of  $V_0$ . In order to make that more concrete, we consider Dysons equation for the system

$$\mathcal{G}(\tau_1, \tau_2) = \mathcal{G}_0(\tau_1, \tau_2) + \int d\tau'' d\tau' \mathcal{G}_0(\tau_1, \tau'') \Sigma(\tau'', \tau') \mathcal{G}(\tau', \tau_2), \quad (4.36)$$

where the Green function is defined as

$$\mathcal{G}(\tau_1, \tau_2) = \begin{pmatrix} \langle T(\gamma_1(\tau_1)\gamma_1(\tau_2)) \rangle & \langle T(\gamma_1(\tau_1)\gamma_2(\tau_2)) \rangle \\ \langle T(\gamma_2(\tau_1)\gamma_1(\tau_2)) \rangle & \langle T(\gamma_2(\tau_1)\gamma_2(\tau_2)) \rangle \end{pmatrix}. \quad (4.37)$$

Due to the inherent particle-hole symmetry of the Majorana fermions we have to consider a matrix Green function. Under the assumption that everything just depends on time differences this can be solved for the Green function in frequency space the usual way. We will then determine  $\Sigma$  such that it gives the same result as the exact Green function for this problem.

We find the exact Green function by first differentiating (4.37) with respect to  $\tau_1$ . This yields

$$\partial_{\tau_1} \mathcal{G}(\tau_1, \tau_2) = 2\delta(\tau_1 - \tau_2) + \begin{pmatrix} 0 & -i\frac{\xi}{2} \\ i\frac{\xi}{2} & 0 \end{pmatrix} \mathcal{G}(\tau_1, \tau_2). \quad (4.38)$$

Where the we used the Schrödinger equation. Note that we have a factor of 2 in front of the delta function, which comes from the normalization of the Majorana fermions. In

#### 4 Perturbative corrections

frequency space we obtain

$$ip_n \mathcal{G}(ip_n) = 2 + \begin{pmatrix} 0 & -i\frac{\varepsilon}{2} \\ i\frac{\varepsilon}{2} & 0 \end{pmatrix} \mathcal{G}(ip_n), \quad (4.39)$$

from which we find

$$\mathcal{G}(ip_n) = 2 \left( ip_n - \begin{pmatrix} 0 & -i\frac{\varepsilon}{2} \\ i\frac{\varepsilon}{2} & 0 \end{pmatrix} \right)^{-1}. \quad (4.40)$$

This has exactly the form of a solution to the Dyson equation of a zero energy Majorana fermion with self-energy

$$\Sigma(ip_n) = \begin{pmatrix} 0 & -i\frac{\varepsilon}{2} \\ i\frac{\varepsilon}{2} & 0 \end{pmatrix}. \quad (4.41)$$

The important thing we take from this result is that, when we calculate the off-diagonal elements of the self-energy, then we associate with them a splitting  $\Delta E$  as follows

$$\Delta E = 2i\Sigma_{12}. \quad (4.42)$$

#### 4.3.2 Phonon Coupling

We will now find the desired Majorana self-energy. We assume that the wire is long enough such that momentum is a good quantum number for phonons. This might easily be the case if the system is longer than the separation between the Majorana fermions. The Majorana fermions can be positioned at domain walls inside the wire away from the edges. This situation is sketched in figure 4.3. We start with the general form of the electron-phonon interaction in momentum space, that is

$$H_I = \sum_q M_q \rho(q) (a_q + a_{-q}^\dagger). \quad (4.43)$$

As before we are only interested in the induced coupling between the Majorana and other electronic states. Therefore we again use  $\tilde{\rho}$  from equation (3.20) for  $\rho$ . In particular we need its Fourier transform which is

$$\tilde{\rho}(k) = \sum_j i\gamma_j \Gamma_{jk}, \quad (4.44)$$

where

$$\Gamma_{jk} = i\frac{1}{2} \int dx e^{ikx} \left( f_j^*(x) \Psi(x) - f_j(x) \Psi^\dagger(x) \right). \quad (4.45)$$

It should be noted that the  $\Gamma_{ik}$  are Majorana mode operators, i.e.  $\Gamma_{ik}^\dagger = \Gamma_{i-k}$ .

With these definitions we can write the reduced interaction Hamiltonian in the following short form

$$\tilde{H}_I = i \sum_{j,k} M_k \gamma_j \Gamma_{j,k} \varphi_k, \quad (4.46)$$

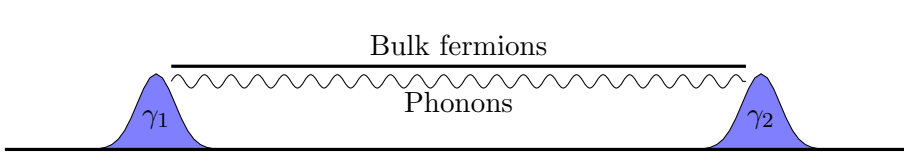


Figure 4.3: Sketch of how phonons that couple the Majorana fermions to the electronic bulk excitations may mediate a Majorana splitting.

where  $\varphi_k = a_k^\dagger + a_k$ . The appearance of the phonon operators prevents us from performing the sum over  $k$  in order to write the interaction in the same form as (3.15). Nonetheless it can easily be seen that the operators  $\Gamma_{jk}$  also fulfill

$$\{\gamma_j, \Gamma_{lk}\} = 0 \quad (4.47)$$

by the same argument as in the earlier case.

### 4.3.3 Self-Energy

The second order correction for the Majorana Green function now looks like

$$\begin{aligned} \mathcal{G}_{12}(\tau) &= - \int d\tau_1 \int d\tau_2 \langle T(\gamma_1(\tau)\gamma_2(0)\tilde{H}_I(\tau_1)\tilde{H}(\tau_2)) \rangle \\ &= \int d\tau_1 \int d\tau_2 \langle T(\gamma_1(\tau)\gamma_1(\tau_1)) \Sigma_{12}(\tau_1, \tau_2) \langle T(\gamma_2(\tau_2)\gamma_2(0)) \rangle \rangle, \end{aligned} \quad (4.48)$$

where we have

$$\Sigma_{12}(\tau_1, \tau_2) = 2 \sum_{k,k'} M_k M_{k'} \langle T(\Gamma_{1k}(\tau_1)\Gamma_{2k'}(\tau_2)) \rangle \langle T(\varphi_k(\tau_1)\varphi_{k'}(\tau_2)) \rangle. \quad (4.49)$$

Because we will only be concerned with the off-diagonal elements of  $\Sigma$  we will drop the subscript 12 on  $\Sigma$ . We can now take a closer look at the  $\Gamma$  correlation function to obtain

$$\langle T(\Gamma_{1,k}(\tau_1)\Gamma_{2,k'}(\tau_2)) \rangle = \frac{1}{4} \int dx dx' e^{ikx} e^{ik'x'} \tilde{f}_1^T(x) \mathcal{G}(x' - x, \tau_2 - \tau_1) \tilde{f}_2(x'), \quad (4.50)$$

where  $\tilde{f}_1^T = (-f_1(x), f_1^*(x))$  and  $\tilde{f}_2^T(x) = (f_2^*(x), -f_2(x))$  and  $\mathcal{G}$  is the matrix Green function defined as follows

$$\mathcal{G}(x - x', \tau_1 - \tau_2) = \begin{pmatrix} \langle T(\Psi^\dagger(x, \tau_1)\Psi(x', \tau_2)) \rangle & \langle T(\Psi^\dagger(x, \tau_1)\Psi^\dagger(x', \tau_2)) \rangle \\ \langle T(\Psi(x, \tau_1)\Psi(x', \tau_2)) \rangle & \langle T(\Psi(x, \tau_1)\Psi^\dagger(x', \tau_2)) \rangle \end{pmatrix} \quad (4.51)$$

Furthermore we recognize the  $\varphi$  correlation function as the phonon Green function

$$\langle T(\varphi_k(\tau_1)\varphi_{k'}(\tau_2)) \rangle = \delta_{k,-k'} \mathcal{D}(k, \tau_2 - \tau_1). \quad (4.52)$$

#### 4 Perturbative corrections

In order to simplify the expression further we go to momentum space using

$$\begin{aligned}
\tilde{f}_1(x) &= \frac{1}{\sqrt{V}} \sum_{p'} e^{ip'x} \tilde{f}_1(p') \\
\tilde{f}_2(x') &= \frac{1}{\sqrt{V}} \sum_{p''} e^{ip''x'} \tilde{f}_2(p'') \\
\mathcal{G}(x' - x, \tau_2 - \tau_1) &= \frac{1}{V} \sum_p e^{ip(x'-x)} \mathcal{G}(p, \tau_2 - \tau_1).
\end{aligned} \tag{4.53}$$

This way the space integrations yield two constraints due to momentum conservation, namely

$$\begin{aligned}
k - p + p' &= 0 \\
-k + p + p'' &= 0.
\end{aligned} \tag{4.54}$$

This way we obtain

$$\langle T(\Gamma_{1,k}(\tau_1)\Gamma_{2,-k}(\tau_2)) \rangle = \frac{1}{4} \sum_p \tilde{f}_1(p-k)^T \mathcal{G}(p, \tau_2 - \tau_1) \tilde{f}_2(k-p). \tag{4.55}$$

Note that this means that  $\Sigma(\tau_1, \tau_2) = \Sigma(\tau_2 - \tau_1)$ .

Finally we want to transform the expressions to frequency space. To this end we use

$$\mathcal{G}(p, \tau_1 - \tau_2) = \frac{1}{\beta} \sum_{p_{n'}} \mathcal{G}(ip_{n'}, p) e^{-ip_{n'}(\tau_1 - \tau_2)} \tag{4.56}$$

and

$$\mathcal{D}(k, \tau_1 - \tau_2) = \frac{1}{\beta} \sum_{\omega_n} \mathcal{D}(i\omega_n, k) e^{-i\omega_n(\tau_1 - \tau_2)}. \tag{4.57}$$

to calculate

$$\begin{aligned}
\Sigma(ip_n) &= \int d\tau \Sigma(\tau) e^{ip_n\tau} \\
&= \frac{1}{2} \sum_{k,p} M_k M_{-k} \tilde{f}_1(p-k)^T B(p, k, ip_n) \tilde{f}_2(k-p)
\end{aligned} \tag{4.58}$$

Here we have

$$\begin{aligned}
B(p, k, ip_n) &= \int d\tau e^{ip_n\tau} \mathcal{G}(p, \tau) \mathcal{D}(k, \tau) \\
&= \frac{1}{\beta^2} \sum_{\omega_n p_{n'}} \int d\tau e^{i(p_n - p_{n'} - \omega_n)\tau} \mathcal{G}(p, ip_{n'}) \mathcal{D}(k, i\omega_n) \\
&= \frac{1}{\beta} \sum_{\omega_n} \mathcal{G}(p, ip_n - i\omega_n) \mathcal{D}(k, i\omega_n).
\end{aligned} \tag{4.59}$$

We are interested in the large  $L$  behavior of equation (4.58). At this point  $L$  does not even explicitly appear inside the equation. This can easily be achieved by shifting the function  $\tilde{f}_2$  such that it is also localized at zero. This shift will then appear as a phase factor of the form  $e^{i(p-q)L}$ . For large  $L$  this will constitute a strongly oscillating factor inside the momentum sums. We expect this to cause the total expression to go to zero for large  $L$ . The problem we are left with is to identify the most prominent contributions. Another way to look at it is to view the momentum sum as a Fourier transform from momentum to  $L$ . This way it becomes clear that the major contributions will come from those parts, whose Fourier transforms have the highest frequency components. Most significant would be the contributions from singularities. This can be understood from the simple example of the Fourier transform of  $\frac{1}{q}$ . Its Fourier transform is given by

$$\int dq \frac{e^{-iqL}}{q} = i\pi \text{sgn}(L). \quad (4.60)$$

This is clearly constant for large  $L$  and the integral does not go to zero even if the oscillations increase as  $L$  increases. We expect singular terms of this form to yield the most significant contributions, we will therefore, in the course of our analysis, neglect contributions that originate from non-singular parts of our sum.

#### 4.3.4 Self Energy in terms of local functions

Before we proceed and calculate  $B$  we take a small detour to write (4.49) in terms of only local functions. This simply means that we define the function

$$\mathcal{P}(x' - x, \tau_2 - \tau_1) = \sum_k e^{ik(x-x')} M_k M_{-k} \mathcal{D}(k, \tau_2 - \tau_1) \quad (4.61)$$

in order to write

$$\Sigma_{12}(\tau_1, \tau_2) = \frac{1}{2} \int dx dx' \tilde{f}_1^T(x) \mathcal{G}(x' - x, \tau_2 - \tau_1) \tilde{f}_2(x') \mathcal{P}(x' - x, \tau_2 - \tau_1). \quad (4.62)$$

According to our earlier discussion the main contribution to the integral will come from the integration region around  $x' - x = L$ . Therefore the behavior of  $\mathcal{P}$  for large distances is also important in addition to the large distance behavior of  $\mathcal{G}$ . Therefore the self-energy will be small if either of the two functions decays rapidly for large values. It is interesting to note that this might not be the case if one looks at Majorana 4-point functions, in particular vertex contributions. We can think of a simple vertex like the ones depicted in figure 4.4. Similar vertex contributions exist where electron and phonon lines are interchanged. It is not hard to see that in this case the main contributions of the Green functions come from their behavior at distances equal to the separation of the Majorana fermions they connect. If they connect the same Majorana fermion this separation is zero and otherwise finite. This means if the Majorana fermions are pairwise equal, we can still have a non-suppressed vertex contribution even if  $\mathcal{G}$  or  $\mathcal{P}$  (but not both) decays rapidly for large distances. In the figure we will have a finite contribution from the first

#### 4 Perturbative corrections

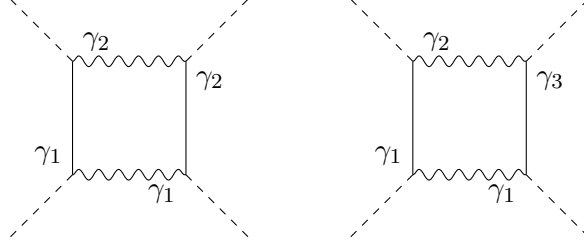


Figure 4.4: Two simple vertex diagrams for Majorana fermions. The wavy lines correspond to phonons, and the solid lines correspond to bulk fermions. The dashed legs only illustrate “outgoing” Majorana fermions. An interchange of phonon and fermion lines also yields valid diagrams.

diagram even if  $\mathcal{G}$  decays rapidly for large distances as long as  $\mathcal{P}$  retains a finite value. If the vertex contains three different Majorana fermions, its contribution is suppressed even if only one of the Green functions is small for large distances, because there at least one fermion and one phonon line that connect different Majorana fermions.

#### 4.4 Calculation of $B$

The first step in calculating the self-energy is now to perform the Matsubara sum in equation (4.59). For this we use the standard phonon Green function

$$\mathcal{D}(k, i\omega_n) = \frac{-2i\omega_k}{\omega_k^2 + \omega_n^2}. \quad (4.63)$$

Furthermore we use the following form for the superconducting Green function

$$\mathcal{G}(p, ip_{n'}) = \frac{-ip_{n'} - H}{p_{n'}^2 + E_p^2}, \quad (4.64)$$

where  $H$  is a particle-hole symmetric translation invariant Hamiltonian. For the lowest-lying band of a translationally invariant superconductor  $\mathcal{G}$  will always take this form. We will justify this form at the end of the section.

Now in order to find the Matsubara sum we have to find the residuals of the function

$$\begin{aligned} f(z) &= n_B(z)\mathcal{D}(k, z)\mathcal{G}(p, ip_n - z) \\ &= n_B(z)\frac{-2i\omega_k}{\omega_k^2 - z^2}\frac{-ip_n + z - H}{E_p^2 - (ip_n - z)^2}, \end{aligned} \quad (4.65)$$

or more precisely we have to find the ones that are not due to  $n_B(z)$ . The poles are easily

seen to be  $\pm\omega_k$  and  $ip_n \pm E_p$ . For the residuals one finds.

$$\begin{aligned}
 z_1 = \omega_k & \quad R_1 = -in_B(\omega_k) \frac{-ip_n + \omega_k - H}{E_p^2 - (ip_n - \omega_k)^2} \\
 z_2 = -\omega_k & \quad R_2 = i(n_B(\omega_k) + 1) \frac{-ip_n - \omega_k - H}{E_p^2 - (ip_n + \omega_k)^2} \\
 z_3 = ip_n + E_p & \quad R_3 = -n_F(E_p) \frac{-2i\omega_k}{\omega_k^2 - (ip_n + E_p)^2} \frac{E_p - H}{2E_p} \\
 z_4 = ip_n - E_p & \quad R_4 = (1 - n_F(E_p)) \frac{2i\omega_k}{\omega_k^2 - (ip_n - E_p)^2} \frac{-E_p - H}{2E_p} \quad (4.66)
 \end{aligned}$$

The function  $B$  is now given by  $B = -(R_1 + R_2 + R_3 + R_4)$ . We will now look at the low frequency limit of the function  $B$ . We will therefore set  $p_n$  to zero. Because  $p_n$  is a fermionic Matsubara frequency it can of course not be exactly zero but can only assume a minimum value of  $\pi k_B T$ . Therefore the temperature has to be low enough such that we can this minimal frequency compared to the relevant energy scales in the denominator. First of all we are going to look at the part of  $B$  that remains at  $T = 0$

$$\begin{aligned}
 B_{T=0}(p, k, 0) & = \frac{-i}{E_p^2 - \omega_k^2} \left[ -\omega_k - H + \omega_k \frac{E_p + H}{E_p} \right] \\
 & = \frac{-i}{E_p^2 - \omega_k^2} \left[ \frac{H(\omega_k - E_p)}{E_p} \right] \\
 & = \frac{iH}{E_p(E_p + \omega_k)}. \quad (4.67)
 \end{aligned}$$

The interesting thing to note about this is that the singular denominator is canceled. We will therefore turn our attention to the parts of  $B$  that remain at finite temperature.

For the temperature dependent part of  $B$  we obtain

$$\begin{aligned}
 B_{T \neq 0}(p, k, 0) & = \frac{-i}{E_p^2 - \omega_k^2} [-n_B(\omega_k)\omega_k - n_F(E_p)\omega_k] \\
 & = \frac{i\omega_k}{E_p^2 - \omega_k^2} [n_B(\omega_k) + n_F(E_p)]. \quad (4.68)
 \end{aligned}$$

This expression still contains the singularity  $E_p = \omega_k$ , which will be of interest to us. It therefore helps to decompose (4.68) into a singular and nonsingular part

$$B_{T \neq 0}(p, k, 0) = \underbrace{\frac{i}{2(E_p - \omega_k)} [n_B(\omega_k) + n_F(E_p)]}_{B_{s,T \neq 0}} - \underbrace{\frac{i}{2(E_p + \omega_k)} [n_B(\omega_k) + n_F(E_p)]}_{B_{ns,T \neq 0}} \quad (4.69)$$

Further discussion will now focus on  $B_{s,T \neq 0}$ .

#### 4.4.1 General form for the electron Green function

We would now like to briefly discuss a general form of the superconducting electron Green function. Our goal is to find the Matsubara Green function for the lowest band of a particle-hole symmetric system. We will first calculate its retarded Green function by solving the equation

$$(\omega + i\eta - H)G_R(\omega) = 1. \quad (4.70)$$

Particle-hole symmetry tells us that for each momentum  $H$  has the solutions  $\pm E_k$  (and only those two since we only consider the lowest band). Therefore when acting on the  $+E_k$  state, the Green function has to take the value  $(\omega + i\eta - E_k)^{-1}$ . On the other hand when acting on the  $-E_k$  state it gives us  $(\omega + i\eta + E_k)^{-1}$ . We can therefore construct the Green function

$$G_R(\omega) = \frac{\omega + i\eta + H}{(\omega + i\eta)^2 - E_k^2} \quad (4.71)$$

that fulfills both those cases and can also be seen to fulfill equation (4.70). From here we can now easily obtain the Matsubara Green function by the replacement  $\omega \rightarrow ip_n$ . This way we obtain

$$\mathcal{G}(p_n) = \frac{-ip_n - H}{p_n^2 + E_k^2} \quad (4.72)$$

#### 4.5 Calculation of $\Sigma$

We would now like to calculate the part of  $\Sigma$  that is due to the singular part of  $B$ , that is

$$\Sigma_s(0) = \frac{1}{2} \sum_{k,p} M_k M_{-k} \tilde{f}_1(p-k)^T B_{s,T \neq 0}(p,k,0) \tilde{f}_2(k-p). \quad (4.73)$$

In order to simplify the equation we first make the  $L$  dependence explicit by replacing  $\tilde{f}_2(q) \rightarrow \tilde{f}_2(q)e^{-iqL}$ . Now both  $f$ s are localized at the same point in real space. Furthermore we will assume that they are localized enough such that we can assume their Fourier transforms to be approximately constant. We then get  $\tilde{f}_1(q)^T \tilde{f}_2(-q) \approx -C \frac{\xi}{V}$ , where  $C$  is some constant of order unity  $\xi$  is the localization length of the Majorana fermions and  $V$  the volume of the system. With those simplifications we get

$$\Sigma_s(0) = -i \frac{C\xi}{4V} \sum_{k,p} M_k M_{-k} \frac{e^{i(k-p)L}}{E_p - \omega_k} [n_B(\omega_k) + n_F(E_p)]. \quad (4.74)$$

Since we assume that the most significant contribution to those sums comes from the singularity, we expand  $\omega_k$  linearly around the  $k$  for which  $E_p = \omega_k$ . This takes the form

$$\omega_k = E_p + a_p(k - k_0(p)). \quad (4.75)$$

Furthermore we assume that the phonon dispersion is symmetric in momentum. We therefore have another contribution from around the point  $-k_0(p)$ . The expansion for this takes the form.

$$\omega_k = E_p - a_p(k + k_0(p)), \quad (4.76)$$

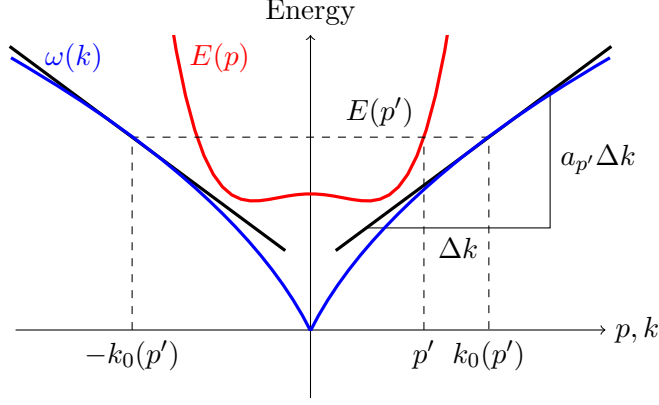


Figure 4.5: For a given value of  $p'$  we can expand we expand  $\omega(k)$  linearly around the points where  $\omega(k) = E(p)$ . Due because we assume  $\omega(k)$  to be an even function of  $k$  there are two (in general an even number) such point  $k_0(p')$  and  $-k_0(p')$ . The slopes at those points are  $a_{p'}$  and  $-a_{p'}$  respectively. We also see that  $k_0(p')$  and  $a_{p'}$  are even functions of  $p'$  if we assume  $E(p)$  to be an even function.

This situation is illustrated in figure 4.5. We now have

$$\begin{aligned} \Sigma_s(0) = & -i \frac{C\xi}{4V} \sum_{k,p} M^2 \left[ \frac{e^{i(k-p)L}}{a_p(k - k_0(p))} [n_B(E_p + a_p(k - k_0(p))) + n_F(E_p)] \right. \\ & \left. - \frac{e^{i(k-p)L}}{a_p(k + k_0(p))} [n_B(E_p - a_p(k + k_0(p))) + n_F(E_p)] \right], \end{aligned} \quad (4.77)$$

where we approximated  $M_k$  by some average value  $M$  around the singularity. Because we expect the main contributions to the sums to come from the singularity. We can then expand the Bose function around that point. In doing so all expansion terms higher then zeroth order will cancel the singularity. For this reason we only keep the zeroth order and get

$$\Sigma_s(0) \approx -i \frac{C\xi}{4V} \sum_{k,p} M^2 \frac{e^{i(k-p)L}}{a_p} n(E_p) \left[ \frac{1}{k - k_0(p)} - \frac{1}{k + k_0(p)} \right], \quad (4.78)$$

where we have  $n(E_p) = n_B(E_p) + n_F(E_p)$ . We will now replace the sums by integrals. First we will perform the  $k$  integration to obtain

$$\begin{aligned} \Sigma_s(0) = & -i \frac{C\xi V M^2}{16\pi^2} \int dk \int dp n_F(E) \frac{e^{i(k-p)L}}{a_p} \left[ \frac{1}{k - k_0(p)} - \frac{1}{k + k_0(p)} \right] \\ = & \frac{C\xi V M^2}{16\pi} \underbrace{\text{sgn}(L)}_1 \int dp \frac{e^{i(k_0(p)-p)L} - e^{i(-k_0(p)-p)L}}{a_p} n(E_p). \end{aligned} \quad (4.79)$$

#### 4 Perturbative corrections

The main contribution to the remaining integral for large  $L$  can be obtained by the stationary phase approximation. This approximation tells us that the main contribution will come from the  $ps$  around the point  $\partial_p(\pm k_0(p) - p) = 0$ . Because we assumed that the Bogoliubov quasi-particle spectrum is symmetric,  $k_0$  is an even function of  $p$  as can be seen from figure 4.5. Therefore  $\partial_p k_0$  is an odd function of  $p$ , which means that if we have  $\partial_p k_0(p_0) = 1$  then we also have  $\partial_p k_0(-p_0) = -1$ . We then get the result

$$\Sigma_s(0) = i \frac{C\xi VM^2}{8\pi} \sqrt{\frac{\pi}{L\partial_p^2 k_0(p_0)}} \frac{\sin((k_0(p_0) - p_0)L + \pi/4)}{a_{p_0}} n(E_{p_0}), \quad (4.80)$$

with which we associate a splitting

$$\Delta E(0) = \frac{C\xi VM^2}{4\pi} \sqrt{\frac{\pi}{L\partial_p^2 k_0(p_0)}} \frac{\sin((k_0(p_0) - p_0)L + \pi/4)}{a_{p_0}} n(E_{p_0}). \quad (4.81)$$

This decays only as  $L^{1/2}$  but is suppressed by the superconducting gap with respect to temperature. It should be noted that the integral does not depend on volume since  $M$  scales as  $V^{-1/2}$ .

We will now look at some of the approximations connected with equation (4.81) in more detail. We expanded  $\omega(k)$  according to (4.75) and (4.76) but then used the formula (4.60) which is only valid if we integrate from  $-\infty$  to  $+\infty$ . The correct way to do this is to restrict the integration range to an area around the singularity. Instead of our simple example(4.60), we would then have to look at

$$\int_{-q_c}^{q_c} dq \frac{e^{-iqL}}{q} = \int dq \frac{\theta(q + q_c) - \theta(q - q_c)}{q} e^{-iqL}. \quad (4.82)$$

In order to calculate this Fourier transform we use the convolution theorem

$$\int dq f(q)g(q)e^{iqL} = \frac{1}{2\pi} \int dx \tilde{f}(x)\tilde{g}(L - x), \quad (4.83)$$

where  $\tilde{f}$  and  $\tilde{g}$  are the Fourier transforms of  $f$  and  $g$  respectively. If we now take  $g(q) = \frac{1}{q}$  we can write the expression as follows

$$\begin{aligned} \int dq \frac{f(q)}{q} e^{iqL} &= \frac{i}{2} \left[ \int_{-\infty}^L dx \tilde{f}(x) - \int_L^{\infty} dx \tilde{f}(x) \right] \\ &= i\pi \left[ \frac{1}{2\pi} \int_{-\infty}^{\infty} dx \tilde{f}(x) - \frac{1}{\pi} \int_L^{\infty} dx \tilde{f}(x) \right] \\ &= i\pi \left[ f(0) - \frac{1}{\pi} \int_L^{\infty} dx \tilde{f}(x) \right]. \end{aligned} \quad (4.84)$$

If we compare this with equation (4.60) we it appears that we have two types of corrections. First of all the limiting value for large  $L$  is changed by a factor  $f(0)$ , but since for us  $f(q) = \theta(q + q_c) - \theta(q - q_c)$  just describes our cutoffs we have  $f(0) = 1$  and we do

not have an overall factor after all. It remains the  $L$  dependent correction of the form  $-\frac{1}{\pi} \int_L^\infty dx \tilde{f}(x)$  to our limiting value. For the Fourier transform of  $f$  we have

$$\begin{aligned} \tilde{f}(x) &= \int dq f(q) e^{iqx} \\ &= q_c \text{sinc} \left( \frac{q_c x}{2\pi} \right), \end{aligned} \quad (4.85)$$

where  $\text{sinc}(x) = \frac{\sin(x)}{x}$ . With this our remaining correction becomes closely related to the sine integral  $\text{Si}(x) = \int_0^x dy \frac{\sin(y)}{y}$ , which is a well studied special function that can be found in [8] for example. From the asymptotic behavior of Si we then find that our correction behaves as  $\frac{\cos(q_c L)}{q_c L}$  for large  $L$ . Therefore we find that regarding the  $k$  cutoffs around equation (4.78) remains valid up to correction of order  $\frac{1}{L}$ .

Another important point is the factor  $n(E_{p_0})$  in the final result. Even though this factor does not change the algebraic  $L$  dependence of equation (4.81) it will be exponentially small in  $\frac{E_{p_0}}{k_b T}$ . The reason why this will yield a particularly small number, is that for this is that we earlier assumed temperature to be low enough such that we could approximately set the fermionic Matsubara frequency to zero. Therefore we are in a low temperature limit. To get a result with a broader applicability, one should keep the Matsubara frequencies. This will move all the poles away from the real line. One could then try to expand the integrals around the parts of the real line that are closest to the poles in the complex plane and hope to capture the Major contribution. This way one might find how contributions from different Matsubara frequencies are suppressed on different length scales. This would give a more complete picture of the system and might also allow one to make some statements about the time evolution of the system because one can in principle attempt Fourier transforms once one knows the self-energy for a relevant range of frequencies.

To briefly summarize this section, we found that electron-phonon coupling may cause a splitting of the Majorana fermion. Within our set of approximations we found that it has an algebraic dependence on the distance between the Majorana fermions, but is exponentially suppressed in temperature.



## 5 Summary

In this thesis we looked at Majorana fermions in quantum wires and qubits that are build out of them.

We described how systems that support Majorana fermions should be composed. Commonly they include  $s$ -wave proximity effect, a strong Zeeman field and spin-orbit coupling. We gave an example for a system that does not rely on spin-orbit coupling, but on a non-homogeneous Zeeman field. For this system we illustrated the connection to the spin-orbit system by means of a position dependent unitary transformation. Furthermore we looked at a concrete example of such a system where the inhomogeneous Zeeman field is generated by an array of magnets. We presented numerical evidence that this system supports Majorana fermions.

We further related the spin-correlation functions for the Majorana qubits to correlation functions of Majorana fermions and used a simple way to classify the topological protection of the individual contributions. This classification consists simply of the rate with which relevant quantities decay in terms of the separation of the Majorana fermions.

Afterwards we analyzed the non-adiabatic effects of time-dependent potentials as an example of non-protected (in our sense) correction. In particular we compared the influence of noise on the correlation function of instantaneous Majorana fermions to the influence of noise to fixed Majorana fermions as it was intensively studied in a paper by Goldstein and Chamon [6]. Furthermore we looked at the effect of uniform motion on the Majorana fermion.

Finally we looked at the splitting for the Majorana fermions that might be caused due to electron-phonon interaction. We found that resonant behavior between phonons and bulk electrons at finite temperature can cause a splitting that decays only as  $L^{-1/2}$  with the separation  $L$  of Majorana fermions. It is however strongly suppressed in temperature on the size of the superconducting gap. This implies that there is no observable splitting due to phonons for sufficiently low temperatures. At higher temperatures some of our approximations loose their validity and we suspect this to cause a different  $L$  behavior. This might be interesting for future investigation.



## 6 Acknowledgments

I would like to thank my supervisor Karsten Flensberg for always being available for questions and very helpful discussions. I would like to thank Piet Brouwer for enabling me to write my master thesis in Copenhagen. I would also like to thank Morten Kjærgaard for valuable discussions and proof reading of this thesis. I would like to thank Jörg Behrmann for repeatedly proof reading this thesis.



## Bibliography

- [1] I. L Aleiner, P. W Brouwer, and L. I Glazman. Quantum effects in coulomb blockade. *arXiv:cond-mat/0103008*, March 2001. Physics Reports, Volume 358, Issues 5-6, March 2002, Pages 309-440.
- [2] Jason Alicea, Yuval Oreg, Gil Refael, Felix von Oppen, and Matthew P. A Fisher. Non-Abelian statistics and topological quantum information processing in 1D wire networks. *arXiv:1006.4395*, June 2010. Nature Physics 7, 412-417 (2011).
- [3] Meng Cheng, Victor Galitski, and Sankar Das Sarma. Non-adiabatic effects in the braiding of Non-Abelian anyons in topological superconductors. *arXiv:1106.2549*, June 2011. Phys. Rev. B 84, 104529 (2011).
- [4] T. -P Choy, J. M Edge, A. R Akhmerov, and C. W. J Beenakker. Majorana fermions emerging from magnetic nanoparticles on a superconductor without spin-orbit coupling. *1108.0419*, August 2011.
- [5] I. C. Fulga, F. Hassler, A. R. Akhmerov, and C. W. J. Beenakker. Scattering formula for the topological quantum number of a disordered multimode wire. *Physical Review B*, 83(15):155429, April 2011.
- [6] Garry Goldstein and Claudio Chamon. Decay rates for topological memories encoded with majorana fermions. *arXiv:1107.0288*, July 2011.
- [7] Alexei Kitaev. Unpaired majorana fermions in quantum wires. *arXiv:cond-mat/0010440*, October 2000.
- [8] N. N. Lebedev and Mathematics. *Special Functions & Their Applications*. Dover Pubn Inc, revised. edition, 1972.
- [9] Roman M Lutchyn, Jay D Sau, and S. Das Sarma. Majorana fermions and a topological phase transition in Semiconductor-Superconductor heterostructures. *arXiv:1002.4033*, February 2010. Phys. Rev. Lett. 105, 077001 (2010).
- [10] PerOlov Lwdin. A note on the QuantumMechanical perturbation theory. *The Journal of Chemical Physics*, 19(11):1396–1401, November 1951.
- [11] Yuval Oreg, Gil Refael, and Felix von Oppen. Helical liquids and majorana bound states in quantum wires. *Physical Review Letters*, 105(17):177002, October 2010.
- [12] M. Wimmer. Efficient numerical computation of the pfaffian for dense and banded skew-symmetric matrices. *arXiv:1102.3440*, February 2011.

## *Bibliography*

- [13] Roland Winkler. *Spin-orbit Coupling Effects in Two-Dimensional Electron and Hole Systems*. Springer Berlin Heidelberg, softcover reprint of hardcover 1st ed. 2003 edition, December 2010.